

PAPER

Prospective life-cycle modeling of a carbon capture and storage system using metal–organic frameworks for CO₂ capture†

Cite this: *RSC Advances*, 2013, 3, 4964

Roger Sathre^a and Eric Masanet^b

Metal–organic frameworks (MOFs) are promising new material media for carbon dioxide (CO₂) capture. Their tunable adsorption patterns may allow relatively efficient separation of gases, e.g. from power plant exhaust. Here we conduct scenario-based prospective life-cycle system modeling to estimate the potentials and implications of large-scale MOF application for post-combustion carbon capture and storage (CCS), and estimate the source and magnitude of uncertainties. The methodological approach includes parametric system modeling to quantify relations between system components; scenario projections of plausible pathways for system scale-up; proxy data on analogous materials and processes; and uncertainty analysis of parameter significance. We estimate the system-wide material and energy flows and economic costs associated with projected large-scale CCS deployment. We compare the performance of a MOF-based system to currently more mature amine-based capture technology. We discuss balancing two critical factors that determine the success of CO₂ capture media: thermodynamic efficiency of the capture/regeneration cycle, and life-cycle embodied energy and cost of the material and its ancillary systems.

Received 3rd November 2012,
Accepted 25th January 2013

DOI: 10.1039/c3ra40265g

www.rsc.org/advances

1 Introduction

Coal fuel was used to produce about 45% of electricity in the United States¹ and 40% of global electricity² in 2010. Because of the large geological reserves of coal in many countries, the well established technologies for using the fuel for electricity generation, and the growing global demand for energy services, it is likely that coal will continue to be used for many years into the future. Carbon capture and storage (CCS) is increasingly discussed as a means to reduce carbon dioxide (CO₂) emissions from coal use and thereby limit climate destabilization. CCS entails separating CO₂ from other gases, compressing and transporting it, and injecting it into deep geologic formations for long-term storage.

There are high expectations for CCS as a strategy for climate change mitigation. For example, Pacala and Socolow³ suggested that CCS could be used to avoid emissions of 11 GtCO₂ y⁻¹ globally by 2054, and IEA⁴ projected that using CCS might avoid emissions of 8 GtCO₂ y⁻¹ globally by 2050. Such quantities would entail a scale-up of 1000 times or more over current global CCS levels of several MtCO₂ y⁻¹, part of which now supports enhanced oil recovery efforts.⁵

Efficient gas separation is a thermodynamic challenge that CCS must overcome if it is to scale up significantly. A medium is needed to selectively capture gas molecules, then release them with modest inputs of energy. Metal–organic frameworks (MOFs) are a novel class of materials with potential for efficient separation of CO₂ from flue gas streams.⁶ MOFs are nanoporous crystalline solids composed of metal-based nodes connected by organic bridging ligands. Their large internal surface area gives them high capacity for gas adsorption, and their pore surfaces can be tuned to enable highly selective binding of CO₂. While showing great promise, MOF research is still at an early stage and significant questions must be resolved for MOF materials to be used for large-scale CO₂ capture.⁷

For technologies such as MOF-based CO₂ capture that are at early stages of development, it is challenging to accurately assess their potential performance at industrial scale. For example, mass, energy, and economic balances may scale in non-linear and diverging ways.⁸ The greater the scale-up ratio from the current experience to the desired plant scale, the more intermediate steps may be required, e.g. bench scale, pilot scale, semi-commercial plant, and commercial plant. At each step, the understanding of system characteristics increases and quantification of inputs and outputs becomes more precise. To estimate the performance of future technologies, it is necessary to identify and bound the potential variability of all critical phenomena and their interactions.

^aEnvironmental Energy Technologies Division, Lawrence Berkeley National Laboratory, Berkeley, California, USA

^bDepartment of Mechanical Engineering, Northwestern University, Evanston, Illinois, USA

† Electronic supplementary information (ESI) available. See DOI: 10.1039/c3ra40265g

In this analysis, we conduct prospective life-cycle modeling of a CCS system using MOF material for CO₂ capture. Our research objectives are to identify the likely bounds of MOF system performance in terms of GHG emission reductions, primary energy use, and economic cost. We compare the estimated future MOF system performance to that of the better-understood amine solvent CO₂ capture process. Using scenario analysis and parametric modeling, we seek to identify critical conditions for the success of large-scale MOF-based systems, as well as risks of failure. Finally, we identify magnitudes and sources of uncertainty, and suggest priority topics for future research. The early-stage life-cycle modeling presented here is intended to generate knowledge to inform decisions made by material scientists (*e.g.* performance targets for laboratory research), process engineers (*e.g.* critical design parameters for system scale-up), and policy makers (*e.g.* GHG mitigation potentials and costs of CCS).

2 Methodology

The field of prospective life-cycle modeling is an emerging research discipline that expands the scope of conventional post-facto LCA techniques. The primary challenge of prospective life-cycle modeling is to credibly describe a system that does not yet exist. In our methodological approach, we create and use a parametric model that quantifies the relations amongst a broad range of system functional components. We integrate data from literature and from the laboratory, and where specific data are unavailable we identify analogous materials and processes to serve as proxies. Data sets include central tendencies and expected ranges. The model is implemented with multiple scenario projections that describe plausible pathways for system scale-up. Throughout, we conduct robust uncertainty analysis to understand the limits of current knowledge and identify further research needs.

A schematic functional diagram of the CCS life-cycle system model is shown in Fig. 1. The model is driven by scenario conditions (1), which determine annual electricity production from various generation technologies through 2050. Power plant modeling (2) determines the required material inputs to, and outputs from, each type of power plant per unit of produced electricity. Coal mining and transport (3) modeling estimates the cost, energy use, and emissions for providing the required quantities of coal fuel. Production and use of conventional monoethanolamine (MEA) (4) is considered as a comparison to more mature CO₂ capture technology. The production of MOF material is modeled by gate-to-gate analysis of MOF synthesis (5), plus cradle-to-gate modeling of solvents (6), organic ligands (7), and metals (8). Recycling feedback loops have mass flow implications for metals (8) and solvents (6). CO₂ transport modeling (9) describes the production, installation, and operation of a pipeline network, including re-compression of CO₂. CO₂ injection modeling (10) describes the production, operation, and monitoring of CO₂ injection wells.

The model incorporates ~60 parameters describing uncertainties (for which the exact value is not known definitively) and variables (which can be varied by design). Each of these parameters is quantified with a “base-case” value, as well as low and high values reflecting the estimated range of the parameter. The range between low and high estimates is indicative of the uncertainty regarding the actual value of the parameter in a large-scale physical system. Parameter values come from experimental data, proxy data on analogous processes, and informed assumptions, as described below. Table S1, ESI† lists the low, middle (base-case) and high estimates for the parameters used in the model.

We estimate the energy and material use and costs of large-scale MOF production by using a hybrid modeling approach integrating bottom-up experimental data from laboratories,

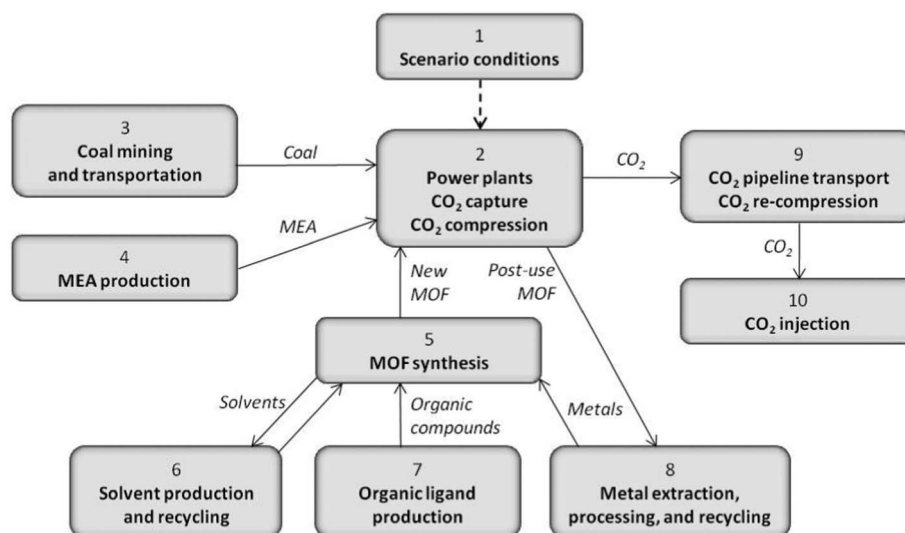


Fig. 1 Schematic functional diagram of the CCS life-cycle system model.

top-down economic data on the US chemical industry, and process data on large-scale manufacture of proxy materials as described below. We use cradle-to-gate (*i.e.* from the extraction of natural resources to the entrance gate of the MOF synthesis plant) production data for raw materials (organic ligands, metals and metal salts, solvents), gate-to-gate (*i.e.* converting raw materials received at the plant entrance into finished products delivered from the plant exit) process data for MOF synthesis, and mass flow modeling of post-use recycling of metals and solvents. Reverse experience curves are applied to estimate the cost profile of MOF production during the scale-up period; future at-scale MOF production cost, based on known current production costs of industrial-scale proxy materials, are adjusted to estimate higher costs of MOF production at early stages of scale-up. We do not consider transportation impacts of new or post-use MOF materials.

We track four primary indicators (primary energy use, GHG emissions, metal use, and monetary cost) and one derived indicator (GHG mitigation cost). Primary energy use includes all energy used throughout the system, including energy inputs for producing and delivering end-use energy forms (*e.g.* electricity generation losses, fuel refining and delivery losses). We comprehensively model the full fuel cycle of coal, and we estimate the primary energy use associated with petroleum and natural gas use based on the higher heating value (HHV) of the end-use fuel plus 5% fuel cycle input.⁹ GHG emission accounting includes CO₂, CH₄, and N₂O emissions from all system components. The latter two species are converted to carbon dioxide equivalent (CO₂e) using 100-year global warming potentials.¹⁰ Two dimensions of metal used for MOF production are estimated: annual rates of primary metal extraction, and total cumulative metal consumption from 2010 to 2050.

Monetary costs are converted to 2010 US dollars based on appropriate producer price index data.¹¹ We do not attempt to harmonize potential differences in costing assumptions (*e.g.* discount rate, service life) between sources of cost information on different system components. To estimate cost dynamics over time, we apply standard experience curves that result in unit cost reductions with increased cumulative installation due to technological learning. Learning rates and application thresholds (Table S1, ESI†) are based largely on IEA-GHG estimates,¹² with values specific to capital and O&M costs of CO₂ capture, compression, transport, and injection.

We derive the GHG mitigation cost as

$$\text{Mitigation Cost} = \frac{\text{Cost}_{\text{CCS}} - \text{Cost}_{\text{NoCCS}}}{\text{Emissions}_{\text{NoCCS}} - \text{Emissions}_{\text{CCS}}} \quad (1)$$

where the numerator describes the difference in total system-wide cost with and without CCS, and the denominator the difference in total system-wide GHG emissions with and without CCS. We calculate the time profile of estimated annual mitigation costs, as well as the average mitigation cost across all years from 2010 to 2050.

In the following ten sub-sections, we briefly describe the approach, assumptions, and data sources for the various parts

of the model, arranged according to the numbering in Fig. 1. Additional documentation is provided as ESI.†

2.1 CCS deployment scenarios

We develop plausible scenarios describing potential development of the US coal-fired power fleet through the year 2050. The net annual production of coal-fired electricity (TWh y⁻¹) follows the projections of the US Energy Information Agency's 2010 Annual Energy Outlook¹³ through the year 2035, then linearly extrapolated to 2050. A baseline scenario without CCS is compared to a CCS deployment scenario. The baseline scenario has gradual improvement of generation efficiency as new capacity is added and retiring power plants are replaced with more efficient units. Projected retirement dates of existing plants are based on US power plant fleet data from Ventyx.¹⁴ The CCS scenario considers deployment of carbon capture technology in all new power plants, plus gradual retrofitting of MOF capture in all non-retiring power plants. CCS deployment is assumed to begin in 2020, and the full fleet is equipped with CCS by 2050. There may be practical constraints (*e.g.* lack of space in the plant facility) to retrofitting some existing power plants with carbon capture equipment, thus the CCS scenario is illustrative and is meant to show the upper bound of carbon capture potential in US coal-fired plants. Fig. S1, ESI† shows annual electricity production in various types of power plants with and without CCS.

2.2 Power plants

We model the technical performance and cost characteristics of three generations of coal-fired Rankine cycle power plants: subcritical, supercritical, and ultra-supercritical. The main difference between these plant types is the temperature and pressure of the steam used to drive the turbines. The energy conversion efficiency of a power plant is higher as the steam temperature and pressure increase.¹⁵ Most current power plants are subcritical, with steam pressure of around 170 bars. The current state-of-the-art is supercritical plants with steam pressure of around 250 bars. The next generation is expected to be ultra-super-critical with even higher steam pressure and temperature, although currently there are constraints on materials performance for *e.g.* turbine blades. In our scenarios we assume for simplicity that all existing US plants in 2010 are subcritical, all plants built from 2011 to 2025 are supercritical, and all plants built after 2025 are ultra-supercritical. For each of those three types of generating technology, we model plants without CO₂ capture, with MEA-based capture, and with MOF-based capture. We assume 90% of flue-gas CO₂ is captured in plants equipped for CCS.

Technical performance estimates for the three generations of power plants without CCS and with MEA CCS are based largely on MIT data.¹⁶ For the plants with MOF-based capture systems, we disaggregate the MIT data and adjust selected values to reflect expected differences between the MEA and MOF capture systems (Fig. S2, ESI†). Fuel use for producing steam to drive turbines varies between the three plant generations, but is assumed to not vary with CO₂ capture technology. Energy use for CO₂ compression is assumed to remain constant per ton of CO₂ compressed. Energy for

auxiliary power requirements such as flue gas pretreatments, blowers, pumps and compressors is assumed to remain constant per unit of coal fuel used. Energy used for regenerating the MOF capture media is based on measured laboratory data¹⁷ and modeled aggregate capture bed performance (Adam Berger, personal correspondence, June 2011). Potential improvements are modeled through parameter variations. The technical performance and cost estimates for subcritical, supercritical, and ultra-supercritical power plants with no CO₂ capture, MEA-based CO₂ capture, and MOF-based CO₂ capture systems under base-case parameter values are detailed in Table S2, ESI†.

Cost estimates for the three generations of power plants without CCS and with MEA CCS are based largely on MIT data.¹⁶ For the plants with MOF-based capture systems, we disaggregate the MIT data and adjust selected cost components to reflect expected physical differences between the MEA and MOF systems (Fig. S3, ESI†). Capital and operation and maintenance (O&M) costs for boilers, turbines, and generators vary based on the amount of coal fuel used (boilers) and the amount of electricity produced (turbines and generators). The capital and O&M costs for flue gas cleaning vary based on the amount of coal fuel used, in the absence of data suggesting higher sensitivity of MOFs to flue gas contaminants and a greater level of flue gas cleaning required. Capital costs for MOF capture systems are roughly assumed to be 50% higher per unit of CO₂ captured due to the physically larger and more complex capture infrastructure (*e.g.* multiple fixed adsorption beds for the MOF systems *vs.* simpler absorber/stripper columns for recirculating MEA solvent). Estimation of O&M costs related to MOF production is described in Sections 2.5 to 2.8. Capital and O&M costs for CO₂ compression vary based on the amount of CO₂ compressed. Cost for CO₂ capture and flue gas cleaning are varied through low and high parameter values to determine the cost significance of these uncertainties. All capital costs calculated by MIT¹⁶ incorporate a carrying charge factor of 15.1%, which we maintain unchanged.

2.3 Coal supply

Energy use and GHG emissions for coal mining and rail transport are based largely on NETL,¹⁸ upon which we vary the transport distance from mines to power plants and the commissioning of new coal mines. We assume for simplicity that all coal is Illinois #6 bituminous coal with a HHV of 25.35 GJ t⁻¹. Coal mine methane emissions are assumed to be 6.9 kg CH₄ t⁻¹ coal.¹⁸ Historical prices of Illinois bituminous coal are based on EIA.¹ Coal cost projections from 2010 to 2035 are based on EIA Annual Energy Outlook,¹³ and we extrapolate linearly from 2036 to 2050. The AEO “reference case” guides our reference coal cost projection, and the AEO “high coal cost case” is used to explore the significance of higher fuel cost on overall system cost. Historical and projected coal prices are shown in Fig. S4, ESI†.

2.4 MEA production and use

For MEA-based capture systems, we base energy use and GHG emissions for MEA manufacture on Ecoinvent¹⁹ and Pehnt & Henkel.²⁰ MEA consumption rate is based on a survey of

relevant studies.^{20–24} MEA cost is based on ICIS price reporting.²⁵

2.5 MOF synthesis

A variety of MOF synthesis methods are described in the literature. The most common is the solvothermal method which involves heating a solution of ligand and metal salt in solvent for hours or days while the reaction occurs.²⁶ Important chemical parameters include pH, concentration of reactants, and temperature.²⁷ Various methods have been suggested to improve the space-time yield and overall efficiency of MOF production. Son *et al.*²⁸ describe a sonochemical method, and Klinowski *et al.*²⁹ a microwave-assisted method, to synthesize MOFs with faster kinetics and higher yields. Mueller *et al.*³⁰ document electrochemical MOF production where metal ions are provided *via* anodic oxidation rather than metal salt dissolution, avoiding potential nitrate and halide safety concerns. Pichon *et al.*³¹ describe a solvent-free mechanochemical synthesis method, and Friščić & Fábíán³² describe a variant of this method called liquid-assisted grinding in which a very small amount of solvent is added to the reaction mixture.

Across this diversity, we estimate performance bounds on industrial-scale final chemical synthesis processes (*i.e.* not including raw material sourcing) using data on gate-to-gate end-use electricity and fuels (*i.e.* only including energy use with the production plant) for manufacturing 36 proxy chemicals using a diverse range of process steps³³ (see Table S3, ESI†). From this energy use data, we estimate CO₂ emissions based on average US electricity grid emission factor and IPCC³⁴ default emission factors for stationary fuel combustion in manufacturing industries. Of the 36 proxy chemicals, we use the mean values of end use energy (GJ per ton of material produced) and CO₂ emission (tCO₂ per ton of material produced) as base case parameter values, and use the minimum and maximum values as low and high parameter values. The large variability in the production processes between the 36 proxy chemicals is expected to accommodate the potential variability among the different MOF synthesis methods. We conducted a primary energy case-study of electrochemical MOF synthesis based on detailed description by Mueller *et al.*,³⁰ the results of which were found to lie within the range of proxy chemicals. We assume that shaping and immobilization of MOF material into a form usable in capture beds is included in the synthesis process.³⁵

We estimate the gate-to-gate manufacturing cost of large-scale MOF production based on census data on shipment value relative to purchased energy and material costs for the “other basic organic chemical manufacturing” sector (NAICS code 32519) of the US chemical industry.³⁶ We estimate production energy costs based on projected average costs from 2010 to 2050 of fuels¹³ and electricity for proxy material production (see Table S3, ESI†). We calculate ratios of total product shipment value to total cost of purchased fuels and electricity, and to total cost of raw materials, for the sector as a whole. We multiply these ratios by the estimated costs of energy and raw materials, and deduct the raw materials costs from the resulting estimates of total shipment value, to estimate gate-to-gate MOF synthesis cost.

2.6 Solvent production and recycling

Most forms of MOF synthesis, including solvothermal and electrochemical methods, require the use of solvents that may include water, methanol, ethanol, dimethylformamide, isopropanol, propanol, and others. We use data from Capello *et al.*³⁷ and Patel³⁸ on energy use and GHG emissions from the manufacture of organic solvents (including the feedstock energy value of the solvent raw materials), and cost data from an internet survey of industrial sales. We model a simplified recycling loop for used solvents that considers mass balance only, and does not include the cost or energy for recycling processes. Energy recovery from non-recycled post-use solvents is not considered.

2.7 Organic ligands

Candidate organic ligand materials include a large range of organic molecules. For industrial scale production, simpler molecules will be preferred over complex molecules, if both deliver the required performance.³⁹ Manufacturing costs will typically be lower for molecules made with fewer synthesis steps that use simple, atom-efficient reactions. Due to the diversity of potential materials and the paucity of life-cycle inventory data on large-scale manufacture of candidate materials, we use proxy data on cradle-to-gate industrial-scale production of 10 benzene-based organic chemicals.³³ Of the 10 proxy chemicals, we use the mean values of energy use (GJ per t of material produced) and GHG emission (tCO₂e per t of material produced) as base case parameter values, and the minimum and maximum values as low and high parameter values (Table S4, ESI†). The feedstock energy is the dominant contributor to total energy use for all 10 materials, while the processing and supply chain energy inputs are relatively low. This suggests that the total energy intensity of other potential ligand materials will not differ significantly from this range, because they will have similar feedstock energy. Recovery of feedstock energy from organic ligand content of post-use MOF material is not considered.

2.8 Metals supply

Candidate metals for MOF production include aluminum (Al), cobalt (Co), chromium (Cr), copper (Cu), iron (Fe), manganese (Mn), nickel (Ni), titanium (Ti), vanadium (V), zinc (Zn), and zirconium (Zr). Depending on the MOF synthesis method, either elemental metal or metal salt is used as raw material. There can be significant variation in the cost and environmental impacts of metal production depending on whether it is in the form of a refined metal or a metal salt, and also on the purity of the metal or salt. We are unaware of any study investigating the effect of purity of metal or metal salt on MOF synthesis yield or quality. Typical metal salts suitable for MOF production include metal oxides, nitrates, sulfates, and chlorides.³⁹ Nitrates may pose a safety hazard as their oxidizing anions may explode when combined with organic linkers. Chlorides may be more corrosive and require higher capital investment for corrosion resistant material handling equipment. Oxides and sulfates may be suitable salts but their lower solubility may be challenging.

Our base-case analysis considers the production of MOF-74(Mg) using magnesium nitrate hexahydrate metal salt as feedstock, and refined magnesium metal as a high parameter value. We chose MOF-74(Mg) due to its relative maturity and associated availability of data in the public domain. In our estimates of metal use, we make a simplifying assumption that all MOFs have the same metal content by mass percent as MOF-74(Mg). Our base-case analysis assumes 95% recycling of metal in post-use MOF material. Because metal supply and demand are global phenomena, for metal use estimates we scale up the MOF CO₂ capture scenarios from the US level to the global level based on projections of US and global generation of coal-fired electricity through 2050.⁴⁰

We use proxy data on cradle-to-gate industrial-scale production of metal salts, largely from the fertilizer industry.^{33,41–43} Data on mining and smelting of elemental metals are taken from Worrell *et al.*⁴⁴ We use USGS data⁴⁵ on metal production rates and reserves, which we convert to masses of elemental metals in cases where metal compounds are produced (see Table S5, ESI†). We use USGS data⁴⁶ on price history of refined metals, supplemented by an internet survey of current prices for various metal salts. The recovery and reuse of metals from post-use MOF material is considered using a simplified mass flow model to determine the mass balance implications of metals recycling *vs.* primary extraction, but does not include the economic or energetic costs for metal re-processing.

2.9 CO₂ transport

Transport of CO₂ from the power plants to the sequestration sites is assumed to use pipelines. We model a simplified network of feeder pipelines delivering compressed CO₂ from the power plants to a series of trunk pipelines, which transport the CO₂ to the injection sites. The length of feeder and trunk pipelines are variable parameters. Diameters of pipelines vary depending on the volume of CO₂ transported by each pipeline, based on Kuby *et al.*⁴⁷ The wall thickness of pipelines is based on Wildbolz,⁴⁸ emissions from steel production are based on Worrell *et al.*⁴⁴ and emissions from pipeline installation are based on NETL.⁴⁹ CO₂ pressure drop during transport is estimated based on Göttlicher,⁵⁰ and re-compression is carried out if needed before sequestration. Electricity use for re-compression is based on Koornneef *et al.*²¹ and we estimate emissions based on average current US electricity grid. Leakage of CO₂ from pipelines is based on IPCC default emission factors for pipeline transport of CO₂ from a capture site to the final storage site.³⁴ The cost of CO₂ transport is based on McKinsey & Company⁵¹ estimates for onshore CO₂ pipeline transport; we assume half of the cost is fixed and half varies linearly with transport distance.

2.10 CO₂ sequestration

Geological sequestration of CO₂ is assumed to occur *via* injection into saline aquifers at an average depth of 1200 m. Quantities of fuel, steel, and cement for injection well construction and operation are based on Singh *et al.*²² Emissions from steel and cement production are based on Worrell *et al.*⁴⁴ The cost of CO₂ injection and monitoring is based on McKinsey & Company⁵¹ estimates for onshore injection into deep saline aquifers; we assume half the cost

Table 1 Estimated base-case primary energy use in 2050 (EJ y^{-1}) and cumulative primary energy use from 2010 to 2050 (EJ) in the US coal-fired power fleet, with no CCS and with CCS using MEA or MOF capture technology

	Energy use in 2050 (EJ y^{-1})			Cumulative energy use, 2010–2050 (EJ)		
	No CCS	MEA CCS	MOF CCS	No CCS	MEA CCS	MOF CCS
Coal fuel energy	22.2	28.3	26.9	979	1078	1053
Coal mining and transport	0.5	0.6	0.6	21.9	24.2	23.6
Plant infrastructure	0.2	0.4	0.4	3.6	5.8	6.3
Capture media production	0	0.5	1.0	0	8.1	15.4
CO ₂ transport and storage	0	0.5	0.5	0	9.3	8.9
Total	23.0	30.4	29.3	1004	1125	1107

is fixed and half varies linearly with injection depth. We do not consider leakage of CO₂ from geologic reservoirs, nor potential constraints in the existence of suitable geologic formations.

3 Results

First we present early-stage energy, GHG, and cost estimates using base-case parameter values. In Section 3.2 we describe estimated resource use and potential material scale-up constraints. In Section 3.3 we describe the magnitude and sources of system uncertainties, identifying particularly sensitive parameters.

3.1 Base-case estimates

If scaled-up across the entire projected US coal-fired electricity fleet, annual MOF production on the order of 1.5 million tons per year would be required by 2050. This corresponds to a MOF consumption rate of about 0.7 kg MOF per t CO₂ captured, substantially less than the modeled base-case MEA consumption rate of 2.5 kg MEA that is degraded and replaced per t CO₂ captured.

Primary energy use increases when CCS is implemented. Table 1 shows the estimated annual primary energy use in 2050 and the cumulative primary energy use from 2010 through 2050. With MOF capture, the annual energy use in 2050 increases by 27%, and cumulative energy use through 2050 increases by 10%, compared to generating the same amount of electricity without CCS. More energy is used for MEA capture due to its higher energy requirements for capture media regeneration; the annual energy use in 2050 increases by 32%, and cumulative energy use through 2050 increases by 12%, compared to the no-CCS case. Focusing on the additional

energy used in the two CCS systems (incremental to that used in the no-CCS case), the higher capture cycle efficiency of the MOF system results in 24% less additional energy use for coal fuel and coal mining and transport than the MEA system. However, the more complex production of the MOF capture media, as well as the manufacture of larger capture infrastructure, together result in 77% more embodied primary energy use in the MOF system than in the MEA system. Because coal fuel to cover the parasitic load of CO₂ capture is the largest single use of additional energy in the CCS systems, the higher capture efficiency of the MOF system results in 15% lower overall additional primary energy use compared to the MEA system. Time profiles of system-wide primary energy use from 2010 to 2050 are shown in Fig. S5, ESL†

Estimated annual GHG emissions in 2050 and cumulative emissions from 2010 through 2050 are shown in Table 2. Net GHG emissions are reduced significantly when either MEA- or MOF-based CCS is employed. Both systems result in a 27% reduction in cumulative emissions through 2050. The annual emissions in 2050 are reduced by 74% for the MOF system and 73% for the MEA system. The emissions from power plant smokestacks, coal mining and transport, and CO₂ transport and storage are reduced more with the MOF system than with the MEA system, due to its great capture cycle efficiency and lower coal use. However, emissions from plant infrastructure and capture media production are greater for the MOF system than the MEA system. Overall, total net emissions are estimated to be slightly lower for the MOF system than the MEA system. Time profiles of system-wide GHG emissions from 2010 to 2050 are shown in Fig. S6, ESL†

The monetary cost of the system is expected to increase significantly when either MOF- or MEA-based CO₂ capture is implemented. Table 3 shows a breakdown of estimated annual

Table 2 Estimated base-case GHG emissions in 2050 ($\text{GtCO}_2\text{e y}^{-1}$) and cumulative GHG emissions from 2010 to 2050 (GtCO_2e) from the US coal-fired power fleet, with no CCS and with CCS using MEA or MOF capture technology

	GHG emissions in 2050 ($\text{Gt CO}_2\text{e y}^{-1}$)			Cumulative emissions, 2010–2050 ($\text{Gt CO}_2\text{e}$)		
	No CCS	MEA CCS	MOF CCS	No CCS	MEA CCS	MOF CCS
Plant stack emissions	1.97	0.25	0.24	86.8	59.0	58.8
Coal mining and transport	0.21	0.27	0.25	9.2	10.1	9.9
Plant infrastructure	0.01	0.02	0.02	0.2	0.3	0.4
Capture media production	0	0.02	0.03	0	0.3	0.6
CO ₂ transport and storage	0	0.03	0.03	0	0.6	0.6
Total	2.20	0.59	0.58	96.2	70.4	70.2

Table 3 Estimated base-case annual cost in 2050 ($\text{G}\$ \text{y}^{-1}$) and cumulative cost from 2010 through 2050 ($\text{G}\$$) for the US coal-fired power fleet, without CCS and with MEA- or MOF-based CCS, with reference coal cost. Costs with high coal cost projections are shown in parentheses

	Cost in 2050 ($\text{G}\$ \text{y}^{-1}$)			Cumulative cost, 2010–2050 ($\text{G}\$$)		
	No CCS	MEA CCS	MOF CCS	No CCS	MEA CCS	MOF CCS
Generation (capital)	41.9	68.9	64.9	634	1131	1062
Generation (non-fuel operation)	20.5	24.6	23.6	836	901	885
Generation (fuel)	40.7 (88.4)	51.8 (112.7)	49.1 (106.8)	1763 (2826)	1943 (3178)	1898 (3090)
Capture (capital)	0	19.2	25.0	0	306	399
Capture (operation)	0	14.5	19.3 (19.4)	0	230	309 (311)
CO ₂ transport and storage	0	22.9 (24.0)	23.1 (24.0)	0	359 (372)	362 (373)
Total	103.1 (150.8)	202.0 (263.8)	205.0 (263.7)	3232 (4296)	4871 (6118)	4915 (6120)

cost in 2050 and cumulative costs from 2010 through 2050, assuming reference coal costs and high coal cost projections. The annual cost in 2050 is estimated to increase by 96% with MEA capture, and by 99% with MOF capture, over the cost of the system without CCS. Cumulative cost through 2050, including capital and operating expenses for electricity production and CO₂ management, is estimated to increase by 51% for the MEA system and 52% for the MOF system, compared to the no-CCS case. With reference coal prices (remaining fairly constant through 2050 at about $\$1.80$ per GJ HHV), the estimated annual cost of the MOF system in 2050 is about 3% more than the MEA system. The significant reduction in coal use due to the higher capture cycle efficiency of the MOF system (shown in Table 1) results in only a minor reduction in cost, while the increased capital and operations costs of the MOF capture system more than outweigh the reduced coal fuel costs. However, with high coal costs (rising to about $\$4.00$ per GJ HHV in 2050), the coal cost savings due to the more efficient MOF capture is more significant, and the cost of the MOF system is about the same as the MEA system. Fig. S7, ESI† shows time profiles of system-wide costs from 2010 to 2050 with reference coal prices.

The trajectories of estimated GHG mitigation cost from 2025 to 2050 are shown in Fig. 2, for MOF and MEA capture systems with reference and high coal price projections. The downward tendency during the initial period is due to technological learning, whereby the marginal unit cost decreases as

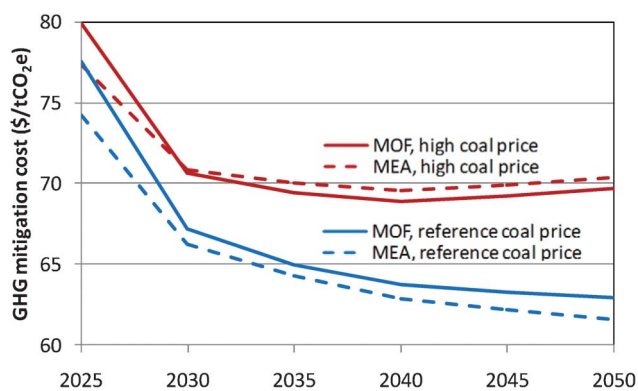


Fig. 2 Estimated GHG mitigation cost ($\$ \text{t}^{-1} \text{CO}_2\text{e}$ avoided emission) trajectory over time for MOF and MEA capture systems, with coal prices based on reference and high coal price projections.

cumulative installed capacity increases.¹² The cost decrease is steeper for MOF capture than for MEA capture because the MEA capture technology is currently at a more advanced stage of development, thus enjoys less benefit from additional technological learning. After the steep initial cost decrease, the mitigation cost continues to decrease slowly with reference coal cost due to the gradually improving efficiencies of CO₂ capture with successive plant generations (see Fig. S1, ESI†). With higher coal costs, the mitigation costs of both MOF and MEA systems remain fairly stable after 2030, because the improving efficiencies are offset by rising coal prices. The estimated average GHG mitigation cost for the MOF system during the entire period is $\$65$ per tCO₂e avoided emission, with reference coal cost. For the MEA system the average mitigation cost is $\$63$ per tCO₂e avoided emission. With high coal cost projection, the estimated average GHG mitigation cost is $\$70$ per tCO₂e avoided emission for both the MOF and MEA systems.

3.2 Resource use

Large scale-up of low-carbon electricity sources may require increased use of metals.⁵² The metal content of the MOF-74(Mg) production modeled here requires a primary Mg metal extraction rate of about $120\,000 \text{ t y}^{-1}$ in 2050, assuming 95% of metal content of post-use MOF materials is recycled. By 2050, half the metal is for new installations and half is to replace recycling losses. After 2050, assuming no new installations (all coal-fired plants are equipped with CCS by 2050, see Fig. S1, ESI†), the annual primary metal requirement stabilizes at about $60\,000 \text{ t y}^{-1}$. When scaled globally based on projected world coal-fired electricity production, the annual primary metal requirement in 2050 is $900\,000 \text{ t y}^{-1}$, or about 14% of current annual global primary Mg extraction. This amount increases if recycling rates are lower than 95%, and decreases if recycling rates are higher than 95% (Fig. S8, ESI†). Assuming constant metal mass percentage in the MOF, the required primary metal extraction rate to enable global scale-up is small relative to current production of Fe, Al, Cu, Mn, Zn, Cr, and Mg (Table 4). Extraction of Ti, Ni, and Zr would have to increase more significantly from current levels to accommodate demands for MOF production. Extraction rates of two metals, Co and V, would have to increase over ten-fold to enable sufficient production of MOFs made with these metals.

To identify potential constraints in total metal supply, the cumulative metal use for global deployment of MOF-based

Table 4 Estimated maximum required extraction rate of various metals for global MOF CCS deployment expressed as percentage of 2010 global primary production of each metal, and cumulative use of various metals for MOF production for global-scale CCS deployment through 2050 expressed as percentage of estimated global reserves of each metal

Metal	Maximum annual metal requirement as percent of 2010 production	Cumulative metal use through 2050 as percent of global reserves
Iron	0.08%	0.02%
Aluminum	2.2%	0.20%
Copper	5.6%	2.3%
Manganese	7.0%	2.3%
Zinc	7.5%	5.9%
Chromium	12%	12%
Magnesium	14%	1.9%
Titanium	23%	3.6%
Nickel	58%	19%
Zirconium	103%	36%
Cobalt	1030%	200%
Vanadium	1620%	110%

CCS through 2050 is compared to the estimated global reserves of various metals, in Table 4. The results are similar to those described above for extraction rates. Cumulative use of most metals (*e.g.* Fe, Al, Mg, Cu, Mn, Ti) for MOF production would be a very small percentage of estimated global reserves of those metals. Use of Zn, Cr, Ni, or Zi would require a somewhat greater percentage of global reserves. Large-scale MOF production with V and Co would require quantities that exceed the estimated global reserves of those metals. An important caveat is that metal “reserves” are defined as the quantity that can be economically extracted given current technology and demand. This amount may vary due to future changes in economic demand or extraction and processing technology. Nevertheless, these results suggest that Co and V (and perhaps also Cr, Zi, and Ni) are poor choices of metals for large-scale MOF production. Higher recycling rates of the metal content in post-use MOF materials would reduce the amount of primary metal required (Fig. S8, ESI†).

In addition to metal supply, other potential resource constraints may affect the scale-up of MOF-based CO₂ capture systems. Manufacture of organic ligands and solvents is generally based on petroleum raw materials, although the feasibility of CO₂ capture with MOFs made from biologically-sourced ligand molecules has been demonstrated.⁵³ While the global supply of petroleum may be expected to contract during the scenario period analyzed here, the quantities of petroleum used for large-scale MOF production would be negligible relative to total petroleum consumption. Another potential resource constraint is water: CO₂ capture generally increases the water use requirements of a power plant, due to the greater need for cooling. A coal plant with conventional carbon capture is estimated to need twice the cooling water of a corresponding plant without CO₂ capture.⁵⁴ A MOF capture system may be physically larger than a MEA system due to the multiple adsorption beds, thus would require more cooling water for rapid temperature swing adsorption cycling. Quantities of water withdrawn *versus* consumed depend on whether once-through or recirculating cooling is used. More

in-depth analysis of water use for MOF CO₂ capture could accompany a preliminary design of capture bed architecture and overall plant cooling system.

3.3 Parameter uncertainty

The significance of individual parameter uncertainty on modeled GHG mitigation cost is shown in Fig. 3. From the base-case condition, each parameter is varied one at a time between its low and high values (Table S1, ESI†), and the effect on mitigation cost is plotted. Significant parameters describing the capture process include capture/regeneration cycle time, life span of MOF material, and the energy needed to regenerate MOF. Significant parameters describing the manufacturing process cluster around solvent management, including the solvent use intensity of MOF synthesis and the solvent recycling rate. Parameter uncertainty is less significant for issues of learning rates, non-solvent production inputs, and CO₂ transport and sequestration.

A significant parameter is the capture/regeneration cycle time, or the time it takes for a capture bed to adsorb CO₂ until saturated, then be purged of CO₂ and be available to adsorb additional CO₂. In temperature swing adsorption systems this parameter depends on heat transfer rates, mass transfer rates, and valving requirements, and determines (in part) the number and size of beds and the quantity of MOF required. This is a very significant parameter and our base case value of 60 min is uncertain. Utilization of pressure swing adsorption regeneration may give faster cycle time than temperature swing adsorption due to heat transfer rate limits, though would come at the cost of additional energy use for vacuum pumps.⁵⁵ A techno-economic analysis weighing the advantages and disadvantages of each system would help illuminate this issue.

Another significant parameter is the MOF lifespan, or the number of capture/regeneration cycles the material can endure before degradation below some minimum performance limit. MOF degradation will depend on its sensitivity to flue gas contaminants, thus requires optimization in parallel with flue gas cleaning equipment. Modeling results suggest that the cost reduction gained by extending the MOF life span from 8000 cycles to 12 000 cycles may be of the same magnitude as a 50% cost increase in flue gas cleaning. However, while costs of flue gas cleaning are fairly well understood, data are lacking on the sensitivity of MOFs to flue gas contaminants. Laboratory-scale testing with simulated flue gas mixtures, followed by pilot-scale slipstream testing at actual power plants, would provide additional knowledge on the degree to which MOF life span may be affected by flue gas contaminants. Regional variation in coal composition may require different optimization solutions for different locations.

The required annual MOF production rate is shown to depend strongly on the capture/regeneration cycle time and the MOF lifespan (Fig. 4). Significantly more MOF production would be needed as lifespan shortens and cycle time lengthens. The system-wide significance of these two uncertain parameters underscores the importance of designing capture/regeneration systems with rapid cycle time, and of producing robust MOFs that are not easily degraded by flue gas contaminants.

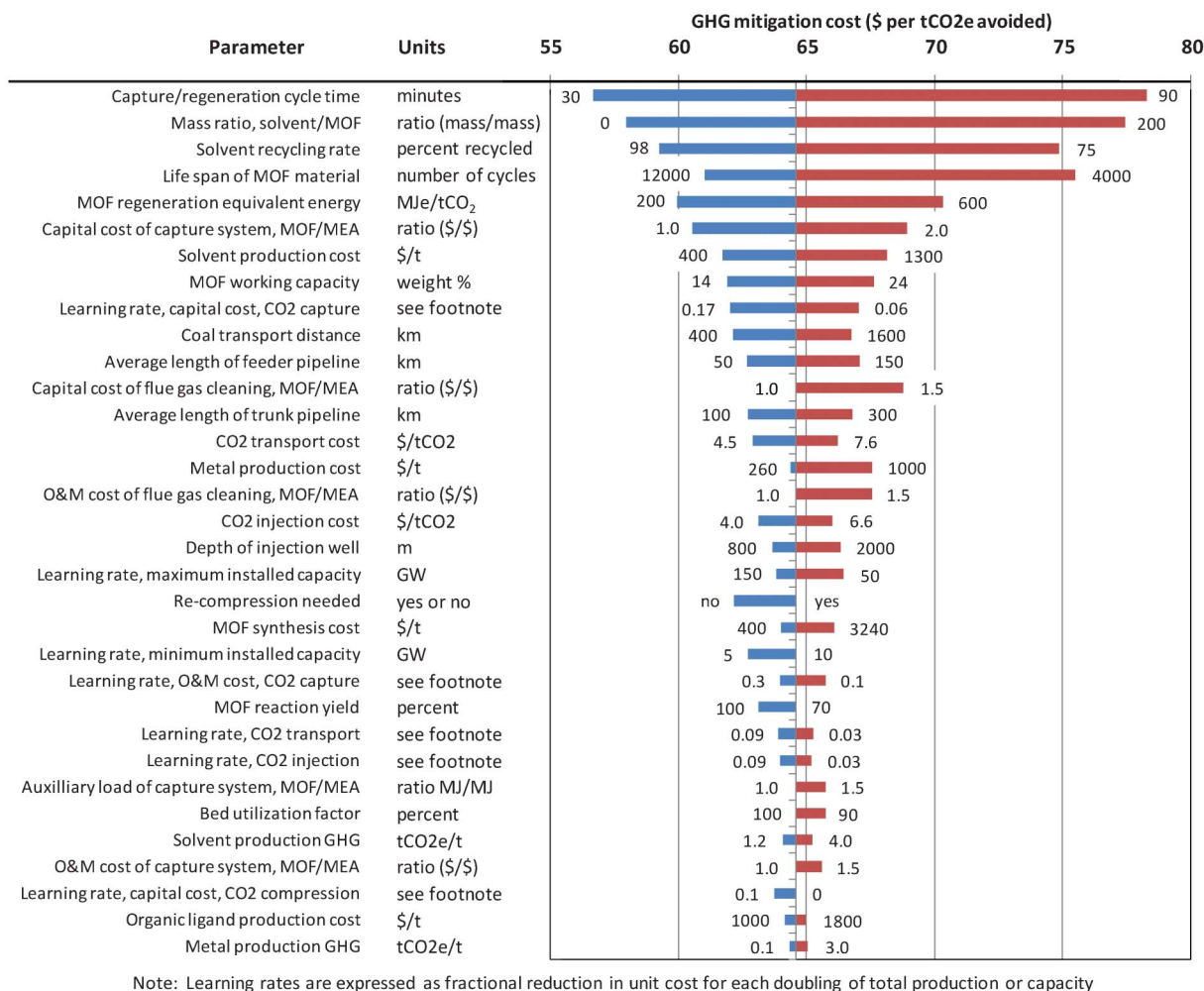


Fig. 3 Change in estimated GHG mitigation cost due to variation of individual parameters between low and high estimates.

Solvent usage for MOF production significantly affects the modeled system performance of MOF-based capture, involving three parameters: solvent intensity of MOF synthesis, solvent recycling rate, and type of solvent. Current laboratory-scale solvothermal and electrochemical MOF synthesis is very

solvent-intensive, requiring up to several hundred grams of solvent per gram of MOF produced. At least one solvent-free synthesis method (mechanochemical) has been reported in the literature,³¹ though its applicability to different MOF types and its feasibility of scale-up are unclear. Solvent-intensive MOF synthesis would be economically untenable at industrial scale without high rates of solvent recycling.³⁹ Feasibility of solvent recycling will depend in part on the type of solvent and the type of contaminants. Solvothermal synthesis using metal salts results in an accumulation of anions in solution, while electrochemical synthesis may in principle avoid accumulation of solvent contaminants. The chemical properties of a particular solvent type may be required to synthesize some MOFs, but where possible the selection of less expensive and less energy-intensive solvents would reduce impacts. In this regard, water would be the preferred solvent, followed in sequence by methanol, ethanol, isopropanol, and DMF.

The amount of energy needed to regenerate CO₂-saturated MOF material is a significant parameter. This is fundamentally based on the temperature-dependent adsorption isotherms of CO₂ and other flue gases such as N₂.¹⁷ Heat energy, most likely in the form of low pressure steam from the power

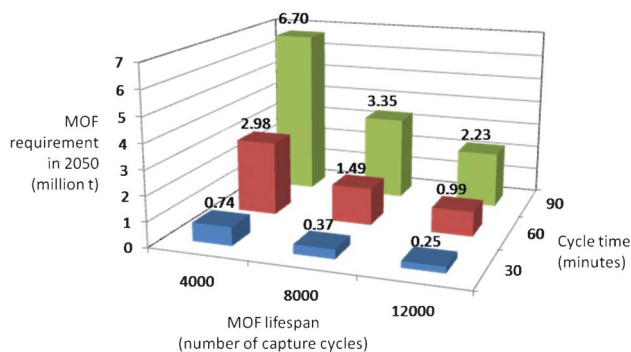


Fig. 4 Estimated amount of required MOF material production in 2050 (million tons y⁻¹) as a function of MOF lifespan and capture cycle time.

plant, is needed to raise the temperature of the media and desorb CO₂ molecules. While efficiencies might be gained by using low grade “waste heat” from power plants, higher heat flows may be needed to maintain a rapid capture/regeneration cycle.⁵⁶ Another model parameter of material properties is MOF working capacity. This describes the amount of CO₂ that is adsorbed by a unit of MOF media during each capture cycle. Expressed as mass percent, our base case working capacity is 18%, which is currently achievable at laboratory scale.¹⁷

The capital cost of a power plant and CO₂ capture equipment is a significant parameter, generally being of a similar magnitude as operational cost. The capital cost for a MOF-based capture installation will depend on the number and size of beds, manifold requirements, and control system, and is likely to be higher than that of an MEA system due to the physically larger and more complex capture infrastructure (e.g. multiple fixed adsorption beds for the MOF systems *versus* simpler absorber/stripper columns for recirculating MEA solvent). Our base case assumption is that capital costs for MOF capture equipment are 50% greater than those of a MEA capture system. This parameter value has large uncertainty and has moderately high impact on the GHG mitigation cost of MOF-based capture. A more detailed techno-economic analysis based on system characteristics is required to better understand this issue and reduce this uncertainty.

Model parameters describing raw material supply and MOF synthesis are less significant. Proxy data on the cost, energy use, and GHG emissions from industrial-scale production of a wide range of chemicals are used in the modeling. This wide range of materials and processes is assumed to encompass the potential range of MOF raw materials and synthesis impacts, and is found to have relatively little effect on overall system performance. The variation in cost, energy use, and GHG emissions among the proxy chemicals, while large in absolute units per ton of material produced, has a small impact per ton of CO₂ emission avoided. Nevertheless, there are uncertainties that would be reduced by further investigation. For example, the required degree of raw material purity for effective industrial-scale MOF synthesis is unclear, and may affect the cost of production. Furthermore, the type of metal that is used for MOF production, as well as the form that metal raw material takes (*i.e.* elemental metal or metal salt), will also affect the costs. Our base-case analysis considers the use of magnesium nitrate hexahydrate (98%) in solvothermal synthesis. The use of elemental Mg metal for electrochemical synthesis would moderately increase the cost. Most metals of interest are less expensive than Mg (e.g. Fe, Mn, Cr, Al, Zn, Zr, Cu), although the use of Co, V, Ti, and Ni would increase the GHG mitigation cost.

The sensitivity results described above are based on variation of one model parameter at a time. We also performed a Monte Carlo simulation to identify interactions among parameters. In this technique, multiple model runs are made, with the values of all uncertain and variable parameters selected for each run based on assigned probability distributions. Summaries of the outcome of 10 000 model runs using triangular probability distributions between high, medium (base-case), and low values for all parameters are shown in Fig. S9, ESI.† For GHG mitigation cost, about one third of the

outcomes lie between \$62 and \$70 per ton of avoided CO₂e emission, and about one half of the outcomes lie between \$60 and \$72. The distribution is skewed with a longer tail toward higher mitigation cost. The outcomes for total cumulative cost and total cumulative primary energy use are similarly skewed. The long tails toward high GHG mitigation cost and total system cost are due in part to the costs of producing large quantities of MOF materials in model runs where values for MOF life span are low and values for capture cycle time are high. Additional variation is introduced by other uncertain parameters such as solvent consumption, MOF regeneration energy, and MOF working capacity. These tails represent unfavorable combinations of key parameter values that must be avoided for MOF-based CCS to be competitive with other CO₂ capture technologies.

4 Discussion and conclusions

The objective of this research is to generate broad insight into the potential environmental, energy, and economic implications of MOF-based CCS systems if implemented at a large scale. Analyzing the effectiveness of GHG emission reduction measures is challenging due to the dynamic nature of the energy system, which includes supply and demand technologies that evolve and expand over time. Analysis at the level of individual power plants provides important technical information on elements of the supply side, but does not put that information in the overall context of the changing energy system.⁵⁷ Here we employ sectoral-level scenario analysis at a larger spatial scale (contiguous US) and temporal scale (2010 through 2050) to provide context for technology development and deployment. To allow objective comparison of the costs and benefits of different options, we use a functional unit defining a time profile of annual net generation of coal-fired electricity (TWh y⁻¹) from 2010 through 2050. This functional unit, a measure of the required outcome of the system, provides the reference to which material, energy, and economic flows are related and compared.

Results from this analysis suggest that two factors should be considered and balanced when optimizing material media for CO₂ capture: 1) the efficiency of the capture/regeneration cycle, and 2) the life-cycle embodied energy and cost of the material and its ancillary systems. The desideratum is a capture medium with high cycle efficiency and low embodied impacts. The capture cycle efficiency will determine the parasitic load of the capture process, which affects the CO₂ mitigation cost *via* the cost of fuel for plant operation (and to a lesser extent to resulting marginal changes in capital cost of plant and fuel supply infrastructure). The life-cycle embodied costs are more diverse, and depend broadly on the supply chain of the capture material including its manufacture and raw material procurement, as well as capital costs for the infrastructure for CO₂ capture.

Our prospective modeling suggests that life-cycle primary energy use may eventually be lower for MOFs than for MEA, mainly because regenerating MOFs may require less energy,

thereby reducing the parasitic load and the associated fuel demand. The overall GHG mitigation effectiveness of MOF and MEA is essentially the same. As modeled using base-case parameter values, MOFs appear to have a slightly higher life cycle cost than MEA, due to the higher capital and operational costs of the MOF capture system. The cost difference between MOF and MEA capture varies with coal price, becoming smaller as coal prices increase.

This modeling exercise has identified a number of uncertain and/or variable parameters that strongly influence the modeled performance of the MOF-based capture system, namely solvent use, media lifespan, capture cycle time, capital cost, regeneration energy, and working capacity. Optimization of one or more of these parameters has the potential to reduce the estimated GHG mitigation cost of MOFs. Future research to explore these key parameters in more depth may allow greater understanding of the potential contribution of MOFs to GHG mitigation and climate stabilization.

The prospective modeling conducted here is intended to provide early information to enable more robust decision making regarding the development and potential use of MOFs for carbon capture. We have endeavored to generate information of use to material scientists, process engineers, and policy makers as they create conditions for a future low-carbon economy. This analysis is offered as a small step toward understanding the potential environmental, energy, and economic implications of large-scale CCS systems. At this early stage, our focus has been to establish ranges of potential outcomes and identify factors that most significantly affect system performance. As additional information becomes available regarding MOF characteristics, additional research should be conducted to expand on these findings and pursue other questions that could not be feasibly addressed in this early-stage investigation.

Acknowledgements

This work was conducted at Lawrence Berkeley National Laboratory under the US Department of Energy Contract No. DE-AC02-05CH11231. The work was funded by the Advanced Research Projects Agency-Energy (ARPA-E), US Department of Energy, under Award No. DE-AR0000103. We thank Jennifer Cain, Mikhail Chester, Kenji Sumida, Adam Berger, Abhoyjit Bhowan, Berend Smit, and Jeff Long for their invaluable assistance.

References

- 1 US Energy Information Agency, *Annual Energy Review*, 2011, <http://www.eia.gov/totalenergy/data/annual/index.cfm>.
- 2 International Energy Agency, *Key World Energy Statistics*, 2012, <http://www.iea.org>.
- 3 S. Pacala and R. Socolow, *Science*, 2004, **305**, 968–972.
- 4 International Energy Agency, *Energy Technology Perspectives 2010: Scenarios and Strategies to 2050*, 2010, <http://www.iea.org>.
- 5 H. J. Herzog, *Energy Econ.*, 2011, **33**(4), 597–604.
- 6 D. M. D'Alessandro, B. Smit and J. R. Long, *Angew. Chem. Int. Ed.*, 2010, **49**, 6058–6082.
- 7 S. Keskin, T. M. van Heest and D. S. Sholl, *ChemSusChem*, 2010, **3**, 879–891.
- 8 A. Bisio and R. L. Kabel, *Scaleup of Chemical Processes*, John Wiley & Sons Inc., New York, 1985.
- 9 C.J. Cleveland, *Energy*, 2005, **30**(5), 769–782.
- 10 Intergovernmental Panel on Climate Change, *Climate Change 2007: The Physical Science Basis. Contribution of Working Group I to the Fourth Assessment Report*, 2007, <http://www.ipcc.ch>.
- 11 US Bureau of Labor Statistics, *Producer Price Index*, 2011, <http://www.bls.gov/data/>.
- 12 International Energy Agency Greenhouse Gas R&D Programme, *Estimating the Future Cost Trends in the Cost of CO₂ Capture Technologies*, IEA-GHG Report Number 2006/6, 2006.
- 13 US Energy Information Agency, *Annual Energy Outlook*, 2010, <http://www.eia.gov/oiaf/archive/aeo10/index.html>.
- 14 Ventyx, *Velocity Suite Database System*, Boulder, 2011.
- 15 J. M. Beér, *Prog. Energy Comb. Sci.*, 2007, **33**(2), 107–134.
- 16 Massachusetts Institute of Technology, *The Future of Coal*, 2007, <http://web.mit.edu/coal/>.
- 17 J. A. Mason, K. Sumida, Z. R. Herm, R. Krishna and J. R. Long, *Energy Environ. Sci.*, 2011, **4**, 3030–3040.
- 18 National Energy Technology Laboratory, *Life Cycle Analysis: Supercritical Pulverized Coal (SCPC) Power Plant*, Report Number DOE/NETL-403-110609, 2010.
- 19 Ecoinvent. *Life Cycle Inventory Database version 2.12010*.
- 20 M. Pehnt and J. Henkel, *Int. J. GHG Control*, 2009, **2**(1), 49–66.
- 21 J. Koornneef, T. van Keulen, A. Faaij and W. Turkenburg, *International Journal of Greenhouse Gas Control*, 2008, **2**(4), 448–467.
- 22 B. Singh, A. Strømman and E. Hertwich, *Int. J. GHG Control*, 2011, **5**(3), 457–466.
- 23 N. Odeh and T. Cockerill, *Energy Policy*, 2008, **36**(1), 367–380.
- 24 A. Korre, Z. Nie and S. Durucan, *Int. J. GHG Control*, 2010, **4**(2), 289–300.
- 25 ICIS Pricing, *Ethanolamines (Europe) Price Report*, 2010, <http://www.icispricing.com>.
- 26 S. T. Meek, J. A. Greathouse and M. D. Allendorf, *Adv. Mater.*, 2011, **23**(2), 249–267.
- 27 G. Férey, *Chem. Soc. Rev.*, 2008, **37**, 191–214.
- 28 W. J. Son, J. Kim, J. Kim and W. S. Ahn, *Chem. Commun.*, 2008, **47**, 6336–6338.
- 29 J. Klinowski, F. A. A. Paz, P. Silva and J. Rocha, *Dalton Trans.*, 2011, **40**(2), 321–330.
- 30 U. Mueller, H. Puetter, M. Hesse, M. Schulbert, H. Wessel, J. Huff and M. Guzmán, *U.S. Patent 7968739*: Method for electrochemical production of a crystalline porous metal-organic skeleton material, 2011.
- 31 A. Pichon, A. Lazuen-Garay and S. L. James, *CrystEngComm*, 2006, **8**(3), 211–214.
- 32 T. Frišćić and L. Fábíán, *CrystEngComm*, 2009, **11**(5), 743–745.
- 33 Energetics Incorporated, *Energy and Environmental Profile of the U.S. Chemical Industry*, Report for the Office of Industrial Technologies, U.S. Department of Energy, 2000.

- 34 Intergovernmental Panel on Climate Change, *IPCC Guidelines for National Greenhouse Gas Inventories*, 2006, <http://www.ipcc-nggip.iges.or.jp/public/2006gl/index.html>.
- 35 B. Böhringer, R. Fischer, M. R. Lohe, M. Rose, S. Kaskel and P. Küsgens, MOF Shaping and Immobilization, Chapter 15 in: *Metal–Organic Frameworks: Applications from Catalysis to Gas Storage*, 2011, ed. D. Farrusseng, Wiley-VCH Verlag GmbH & Co.
- 36 US Census Bureau, *Statistics for Industry Groups and Industries*, 2006, <http://www.census.gov/prod/2006pubs/am0531gs1.pdf>.
- 37 C. Capello, G. Wernet, J. Sutter, S. Hellweg and K. Hungerbühler, *Int. J. Life Cycle Ass.*, 2009, **14**, 467–479.
- 38 M. Patel, *Energy*, 2003, **28**, 721–740.
- 39 A. Czaja, E. Leung, N. Trukhan and U. Müller, Industrial MOF Synthesis, Chapter 14 in: *Metal–Organic Frameworks: Applications from Catalysis to Gas Storage*, ed. D. Farrusseng, 2011, Wiley-VCH Verlag GmbH & Co.
- 40 US Energy Information Agency, *International Energy Outlook*, 2010, <http://www.eia.gov/oiaf/ieo/index.html>.
- 41 J. Davis and C. Haglund, *Life Cycle Inventory (LCI) of Fertiliser Production: Fertiliser Products Used in Sweden and Western Europe*, 1999, SIK-report No. 654.
- 42 M.G. Bhat, B.C. English, A.F. Turhollow and H.O. Nyangito, *Energy in Synthetic Fertilizers and Pesticides: Revisited*, Report ORNL/Sub/90-99732/2, Oak Ridge National Laboratory, 1994.
- 43 T. O. West and G. Marland, *Ag. Ecosyst. Environ.*, 2002, **91**(1–3), 217–232.
- 44 E. Worrell, R. J. J. van Heijningen, J. F. M. de Castro, J. H. O. Hazewinkel, J. G. de Beer, A. P. C. Faaij and K. Vringer, *Energy*, 1994, **19**(6), 627–640.
- 45 US Geological Survey, *Mineral Commodity Summaries*, 2011, <http://minerals.usgs.gov/minerals/pubs/mcs/2011/mcs2011.pdf>.
- 46 US Geological Survey, *Historical Statistics for Mineral and Material Commodities in the United States*, 2010, <http://minerals.usgs.gov/ds/2005/140/>.
- 47 M.J. Kuby, R.S. Middleton and J.M. Bielicki, *Energy Procedia*, 2011, **4**, 2808–2815.
- 48 C. Wildbolz, Diploma Thesis No. 2007MS05, Swiss Federal Institute of Technology, Zurich, 2007.
- 49 National Energy Technology Laboratory, *Life Cycle Analysis: Existing Pulverized Coal (EXPC) Power Plant*, Report Number DOE/NETL-403-110809, 2010.
- 50 G. Göttlicher, *The Energetics of Carbon Dioxide Capture in Power Plants*, NETL, 2004.
- 51 McKinsey & Company, *Carbon Capture and Storage: Assessing the Economics*, 2008.
- 52 R. Kleijn, E. van der Voet, G.J. Kramer, L. van Oers and C. van der Giesen, *Energy*, 2011, **36**(6), 5640–8.
- 53 J.J. Gassensmith, H. Furukawa, R.A. Smaldone, R.S. Forgan, Y.Y. Botros, O.M. Yaghi and J. F. Stoddart, *J. Am. Chem. Soc.*, 2011, **133**(39), 15312–15315.
- 54 H. Zhai, E.S. Rubin and P.L. Versteeg, *Environ. Sci. Technol.*, 2011, **45**(6), 2479–2485.
- 55 R. Willis, *Carbon Dioxide Removal from Flue Gas Using Microporous Metal Organic Frameworks: Final Technical Report*, 2010, <http://www.netl.doe.gov/technologies/coal-power/ewr/co2/pubs/43092F1.pdf>.
- 56 K. Z. House, C. F. Harvey, M. J. Aziz and D. P. Schrag, *Energy Environ. Sci.*, 2009, **2**, 193–205.
- 57 R. Sathre, M. Chester, J. Cain and E. Masanet, *Energy*, 2012, **37**(1), 540–548.

Supplementary Information

Prospective Life-cycle Modeling of a Carbon Capture and Storage System Using Metal-Organic Frameworks for CO₂ Capture

Roger Sathre and Eric Masanet

<http://dx.doi.org/10.1039/c3ra40265g>

Tables

Table S1. Low, middle (base-case), and high estimates of key model parameters.

Table S2. Base-case performance and cost data for three generations of power plants with no CO₂ capture and with MEA- and MOF-based capture systems.

Table S3. Energy use, CO₂ emissions, and energy cost per ton of material, for gate-to-gate processing of 36 proxy materials. Feedstock energy and supply chain energy is not included.

Table S4. Primary energy use and GHG emissions associated with cradle-to-gate production of 10 organic materials.

Table S5. Estimated global mine production and global reserves of various metals in 2010 (USGS 2011). In cases where end-use is a metal compound, we converted mass to elemental metal.

Figures

Figure S1. Illustrative scenarios of US coal-fired electricity production from 2010 to 2050 with three successive generations of efficiency technologies, without CCS (top) and with CCS deployed in retrofitted and new power plants (bottom).

Figure S2. Framework for energy use modeling of power plants with MOF capture.

Figure S3. Framework for cost modeling of power plants with MOF capture.

Figure S4. Historical and projected coal prices (\$ GJ⁻¹). Coal is Illinois bituminous with HHV ≈ 25.35 GJ t⁻¹.

Figure S5. System-wide primary energy use (EJ y⁻¹) from 2010 to 2050 for cases with no CO₂ capture and with MOF- and MEA-based capture systems.

Figure S6. System-wide GHG emissions (million tCO₂e y⁻¹) from 2010 to 2050 for cases with no CO₂ capture and with MOF- and MEA-based capture systems.

Figure S7. Total system cost (G\$ y⁻¹) from 2010 to 2050 for cases with no CO₂ capture and with MOF- and MEA-based capture systems.

Figure S8. Annual primary metal requirement for MOF production, expressed as a percentage of 2010 primary magnesium production, as a function of recycling rate of metal in post-use MOF material.

Figure S9. Outcomes of Monte Carlo simulation of full-scale deployment of MOF-based carbon capture and storage in the US coal-fired power fleet through 2050: GHG mitigation cost (\$ per tCO₂e), total cumulative primary energy use (EJ), total cumulative GHG emissions (Gt CO₂e), and total cumulative cost for coal-fired electricity production (G\$).

Table S1. Low, middle (base-case), and high estimates of key model parameters.

Parameter	Unit	Low	Middle	High
Coal supply				
Coal from newly constructed mines	percent	20%	50%	80%
Coal transport distance	km	400	1000	1600
MEA capture				
MEA consumption	kg per tCO ₂ captured	1.50	2.50	4.00
MEA cost ^a	\$ per t	1275	1700	2125
MEA production GHG emissions	tCO ₂ e per t	2.6	3.4	4.3
MOF capture				
MOF working capacity ^b	percent	14%	18%	24%
MOF regeneration energy	MJe/tCO ₂	200	400	600
Capture/regeneration cycle time	minutes	30	60	90
Life span of MOF	number of capture cycles	12000	8000	4000
Relative capture auxiliary load, MOF/MEA ^c	percent	100%	100%	150%
Capture bed utilization factor	percent	100%	100%	90%
Organic ligand cost	\$ per t	1000	1400	1800
Organic ligand production energy	GJ per t	50	68	96
Organic ligand production GHG	tCO ₂ e per t	0.2	1.3	3.2
Metal cost ^d	\$ per t	260	300	1000
Metal production energy	GJ per t	0.9	8.3	20.9
Metal production GHG	tCO ₂ e per t	0.1	1.0	3.0
Recycling rate for metal in post-use MOF	percent	99%	95%	80%
Solvent cost	\$ per t	400	800	1300
Solvent production energy	GJ per t	45	75	100
Solvent production GHG	tCO ₂ e per t	1.2	2.4	4
Mass ratio, solvent/MOF	ratio	0	70	200
Solvent recycling rate	percent	98%	90%	75%
MOF synthesis cost	\$ per t	400	940	3240
MOF synthesis energy	GJ per t	0.27	15	61
MOF synthesis GHG	tCO ₂ e per t	0.02	0.88	3.6
MOF synthesis reaction yield	percent	100%	85%	70%
CO₂ transport and storage				
Length of feeder line from plant to trunk line	km	50	100	150
Length of trunk line to sequestration site	km	100	200	300
Compression pressure	bar	160	150	140
Wall thickness of pipeline	mm	15	18	21
CO ₂ leakage	t CO ₂ per year per km pipeline	0.14	1.4	14
Downstream re-compression needed	yes or no	no	yes	yes
Baseline transport cost	\$ per tCO ₂ transported	4.5	6.0	7.6
Baseline injection cost	\$ per tCO ₂ injected	4.0	5.3	6.6
Depth of injection well	m	800	1200	2000
Costs of MOF system relative to MEA system				
Capital cost of flue gas cleaning, MOF/MEA	percent	100%	100%	150%
Capital cost of capture system, MOF/MEA	percent	100%	150%	200%
O&M cost of flue gas cleaning, MOF/MEA	percent	100%	100%	150%
O&M cost of capture system, MOF/MEA	percent	100%	100%	150%
Learning rates				
Learning rate, capital cost, generation	^e	0.09	0.06	0.03
Learning rate, O&M cost, generation	^e	0.3	0.15	0.07
Learning rate, capital cost, flue gas cleaning	^e	0.18	0.12	0.06
Learning rate, O&M cost, flue gas cleaning	^e	0.3	0.22	0.1
Learning rate, capital cost, CO ₂ capture (MEA)	^e	0.17	0.11	0.06
Learning rate, O&M cost, CO ₂ capture (MEA)	^e	0.3	0.22	0.1
Learning rate, capital cost, CO ₂ capture (MOF)	^e	0.17	0.11	0.06
Learning rate, O&M cost, CO ₂ capture (MOF)	^e	0.3	0.22	0.1
Learning rate, capital cost, CO ₂ compression	^e	0.1	0	0
Learning rate, O&M cost, CO ₂ compression	^e	0.1	0	0
Learning rate, CO ₂ transport	^e	0.09	0.06	0.03
Learning rate, CO ₂ injection	^e	0.09	0.06	0.03
Learning rate, minimum installed capacity	GW	5	10	10
Learning rate, maximum installed capacity	GW	150	100	50

Learning rate, maximum cumulative transport	Gt-km	390	260	130
Learning rate, maximum cumulative injection	MtCO ₂	4500	3000	1500

^a High/low values are plus/minus 25% of base-case value

^b Mass of recoverable CO₂ per cycle, as a percentage of the mass of the MOF material

^c Auxiliary energy load (for pumps, fans, etc.) of MOF capture system relative to MEA capture system

^d Middle cost value is for magnesium nitrate hexahydrate (98%) as feedstock; High cost value is for refined magnesium metal, adjusted to account for lower elemental metal content in base-case metal salt

^e Learning rates are expressed as fractional reduction in unit cost for each doubling of total production or capacity

Table S2. Base-case performance and cost assumptions for three generations of power plants with no CO₂ capture and with MEA- and MOF-based capture systems.

	Sub-critical			Super-critical			Ultra-super-critical		
	No capture	MEA capture	MOF capture	No capture	MEA capture	MOF capture	No capture	MEA capture	MOF capture
Heat rate (MJ/MWh)	10498	14349	13353	9359	12344	11574	8314	10551	10007
--Turbines	10498	10498	10498	9359	9359	9359	8314	8314	8314
--Capture media regeneration	0	2093	1219	0	1623	938	0	1216	725
--CO ₂ compression	0	1465	1363	0	1136	1065	0	851	807
--Auxiliary capture loads	0	293	273	0	227	213	0	170	161
Generating efficiency (% HHV)	34.3	25.1	26.9	38.5	29.3	31.2	43.3	34.1	35.8
Coal feed (t/MWh)	0.41	0.57	0.53	0.37	0.49	0.46	0.33	0.42	0.39
CO ₂ emitted (t/MWh)	0.93	0.13	0.12	0.83	0.11	0.10	0.74	0.09	0.09
CO ₂ captured (t/MWh)	0.00	1.15	1.07	0.00	0.98	0.92	0.00	0.84	0.80
Levelized capital costs (¢/kWh)									
Boiler/turbine/generator	0.00 ^a	0.00 ^a	0.00 ^a	2.63	3.26	3.05	2.69	3.18	3.02
Flue gas cleaning	0.00	0.63	0.58	0.49	0.60	0.56	0.50	0.59	0.56
CO ₂ capture	0.00	0.94	1.31	0.00	0.90	1.27	0.00	0.88	1.25
CO ₂ compression	0.00	0.21	0.19	0.00	0.20	0.19	0.00	0.20	0.19
Levelized O&M costs(¢/kWh)									
Boiler/turbine/generator	0.50	0.61	0.56	0.50	0.61	0.57	0.50	0.61	0.57
Flue gas cleaning	0.36	0.44	0.41	0.36	0.44	0.41	0.36	0.44	0.41
CO ₂ capture w/o media	0.00	0.34	0.32	0.00	0.34	0.32	0.00	0.34	0.32
CO ₂ capture media	0.00	0.44	0.63	0.00	0.44	0.63	0.00	0.44	0.63
CO ₂ compression	0.00	0.04	0.04	0.00	0.04	0.04	0.00	0.04	0.04
Fuel costs (¢/kWh)									
Fuel cost in 2010	1.90	2.60	2.42	1.70	2.23	2.09	1.51	1.91	1.82
Fuel cost in 2050 (reference)	1.92	2.63	2.44	1.71	2.25	2.11	1.52	1.93	1.83
Fuel cost in 2050 (high)	4.17	5.71	5.31	3.72	4.90	4.59	3.30	4.20	3.98

^a Capital costs of existing plants are assumed to be fully amortized.

Table S3. Energy use, CO₂ emissions, and energy cost per ton of material, for gate-to-gate processing of 36 proxy materials. Feedstock energy and supply chain energy is not included.

Material	Primary energy ^a (GJ per ton)	CO ₂ emissions ^b (ton CO ₂ per ton)	Energy cost ^c (\$ per ton)
Ethylene	20.8	1.25	157
Polyethylene	7.0	0.38	34
Ethylene Dichloride	9.6	0.57	68
Polyvinyl Chloride	4.1	0.24	27
Ethylene Oxide	6.4	0.36	39
Ethylene Glycol	7.3	0.42	46
Polyester	33.6	2.00	242
Propylene	4.3	0.25	29
Polypropylene	2.1	0.12	12
Propylene Oxide	8.2	0.48	54
Acrylonitrile	3.0	0.18	20
Acrylic Fibers	60.7	3.60	433
BTX	3.3	0.20	25
Benzene	2.9	0.17	22
Ethylbenzene	3.5	0.21	27
Styrene	39.2	2.39	315
Polystyrene	5.9	0.36	44
Cumene	1.7	0.10	13
Phenol/Acetone	20.1	1.21	152
Terephthalic Acid	7.1	0.40	42
Cyclohexane	4.8	0.28	35
Adipic Acid	49.1	2.91	351
Caprolactam	35.1	2.10	259
Nylon 6,6	55.6	3.24	366
Nylon 6	34.0	2.01	236
Chlorine/Sodium Hydroxide	42.2	2.33	216
Sodium Carbonate	8.5	0.51	65
Ammonia	32.6	1.87	214
Urea	2.5	0.15	17
Nitric Acid	0.6	0.04	5
Ammonium Nitrate	1.4	0.08	8
Ammonium Sulphate	12.8	0.74	85
Sulfuric Acid	0.3	0.02	1
Phosphoric Acid	5.8	0.34	38
Ammonium Phosphate	1.1	0.07	7
Superphosphate	3.2	0.18	18
Mean	15.0	0.88	103
Minimum	0.27	0.02	1.4
Maximum	60.7	3.60	433

^a End-use fuels and primary energy associated with end-use electricity used within the production facility (Reference 33). Energy export from exothermic processes, feedstock energy value, and raw material supply chain energy use is not included.

^b CO₂ emissions from energy use. Fuel emissions based on IPCC default emission factors for stationary fuel combustion in manufacturing industries (Reference 34). Electricity emissions based on average US electricity grid emission intensity in 2008.

^c Cost of end-use fuels and electricity in 2010 dollars, based on projected average cost from 2010 to 2050 of fuels (Reference 13) and electricity (calculated within the model).

Table S4. Primary energy use and GHG emissions associated with cradle-to-gate production of 10 organic materials.

Material	Primary energy use (GJ per ton) ^a				GHG emissions (tCO ₂ e/t) ^b
	Process energy	Feedstock energy	Raw material supply chain	Total embodied energy	
BTX	3.3	74.3	0.9	78.5	0.24
Cyclohexane	4.8	49.3	3.9	57.9	0.39
Benzene	2.9	54.1	1.0	58.1	0.25
Ethylbenzene	3.5	44.2	6.9	54.6	0.69
Styrene	39.2	46.6	10.4	96.2	3.18
Cumene	1.7	44.3	3.7	49.7	0.24
Phenol/Acetone	20.1	35.1	5.1	60.3	1.59
Terephthalic acid	7.1	43.7	2.1	52.9	0.56
Adipic acid	49.1	33.5	3.4	85.9	3.17
Caprolactam	35.1	48.8	4.9	88.8	2.47
Mean	16.7	47.4	4.2	68.3	1.28
Minimum	1.7	33.5	0.9	49.7	0.24
Maximum	49.1	74.3	10.4	96.2	3.18

^a Primary energy use based on Reference 33

^b GHG emissions are based on average US electricity grid emission factor and IPCC default emission factors for stationary fuel combustion in manufacturing industries (Reference 34). Emissions from raw material supply chain assume diesel fuel is used for mining, drilling, transportation, etc. No emissions are assigned to feedstock energy.

Table S5. Estimated global mine production and global reserves of various metals in 2010 (Reference 45). In cases where end-use is a metal compound, we converted mass to elemental metal.

Metal	Global mine production (million tons per year)	Global reserves (million tons)	Major mine producing countries
Aluminum	41.4	7409	China, Russia, USA
Chromium	7.6	120	South Africa, Kazakhstan, India
Cobalt	0.088	7	Congo, Zambia, China
Copper	16.2	630	Chile, Peru, USA
Iron	1130 ^a	87000	China, Brazil, Australia
Manganese	13.0	630	China, Australia, South Africa
Magnesium	6.3 ^a	775 ^b	China, Russia, Israel
Nickel	1.6	76	Russia, Indonesia, Philippines
Titanium	3.9	414	China, Japan, Russia
Vanadium	0.056	14	China, South Africa, Russia
Zinc	12.0	250	China, Peru, Australia
Zirconium	0.88	41	Australia, South Africa, USA

^a 2008 data

^b Data from: S.E. Kesler, *Mineral Resources, Economics, and the Environment*, Macmillan College Publishing, New York, 1994.

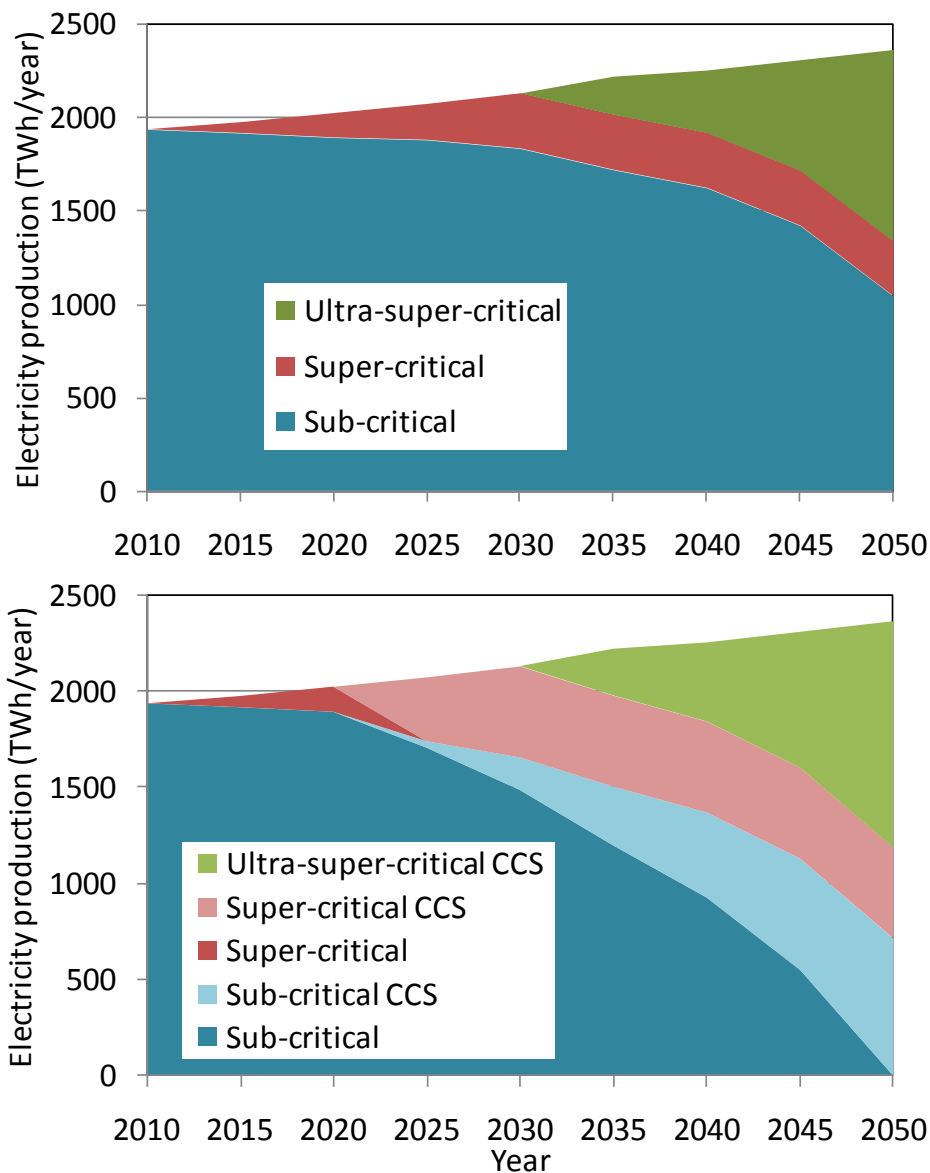


Figure S1. Illustrative scenarios of US coal-fired electricity production from 2010 to 2050 with three successive generations of efficiency technologies, without CCS (top) and with CCS deployed in retrofitted and new power plants (bottom).

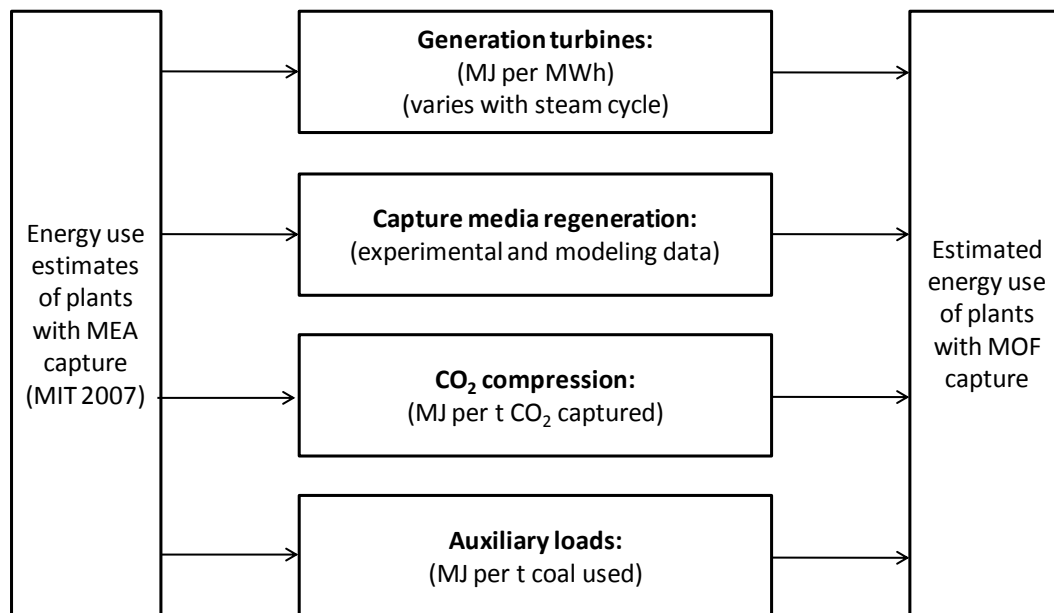


Figure S2. Framework for energy use modeling of power plants with MOF capture.

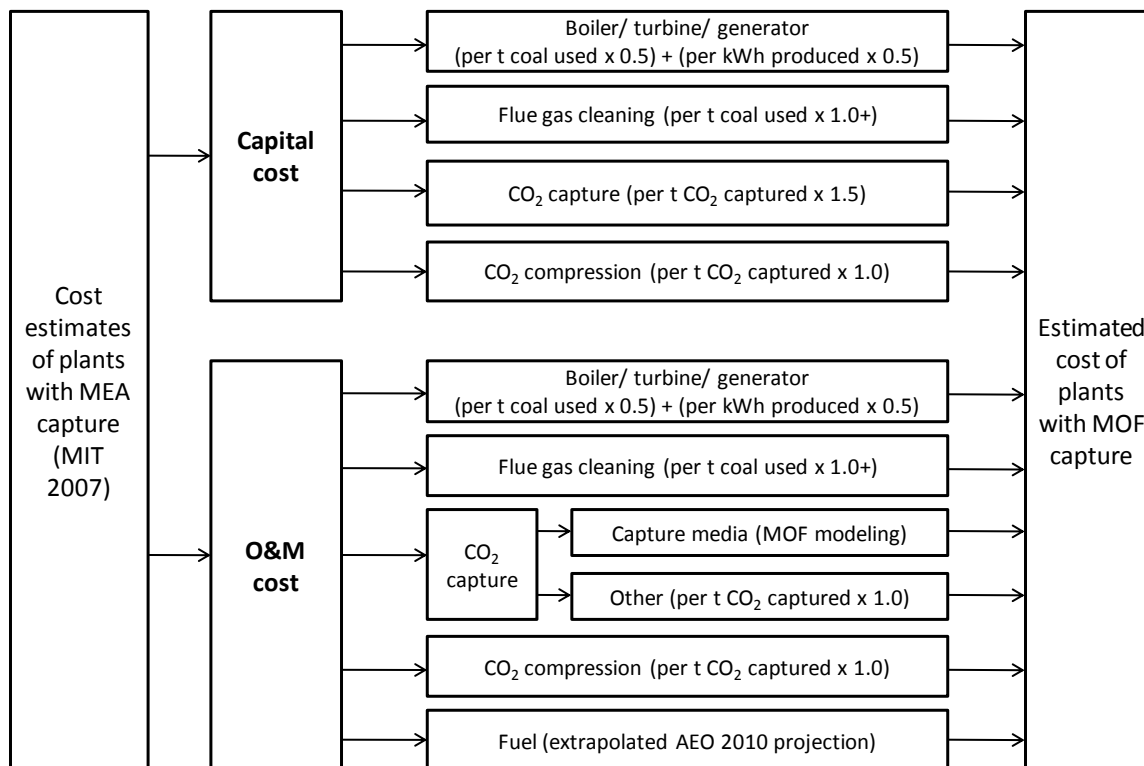


Figure S3. Framework for cost modeling of power plants with MOF capture.

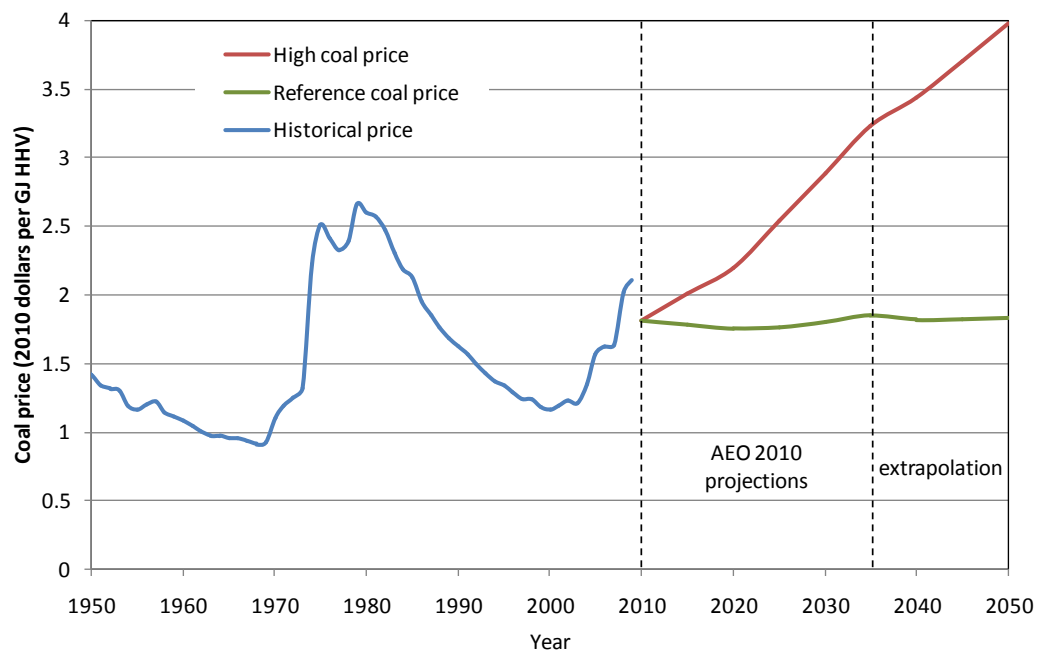


Figure S4. Historical and projected coal prices (\$ GJ⁻¹). Coal is Illinois bituminous with HHV \approx 25.35 GJ t⁻¹.

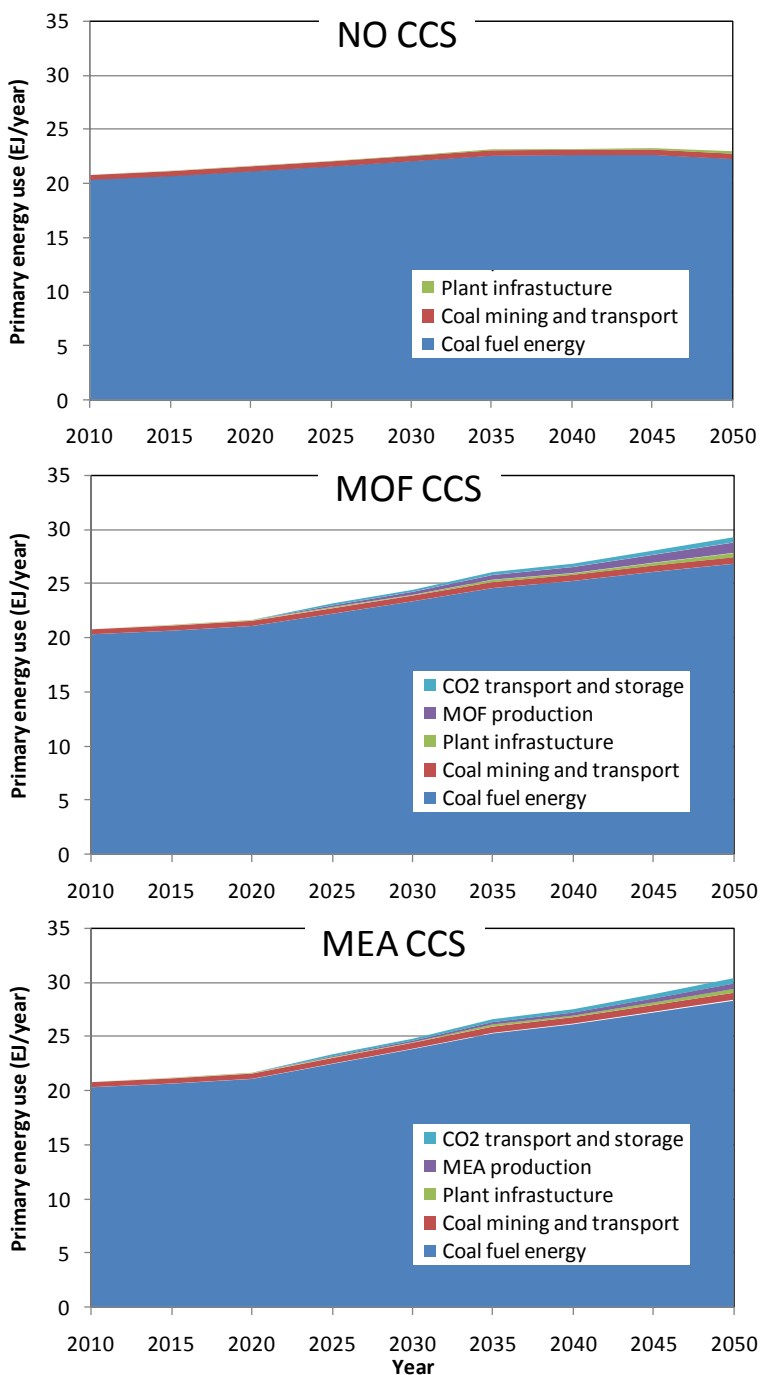


Figure S5. Estimated system-wide primary energy use (EJ y^{-1}) from 2010 to 2050 for cases with no CO_2 capture and with MOF- and MEA-based capture systems.

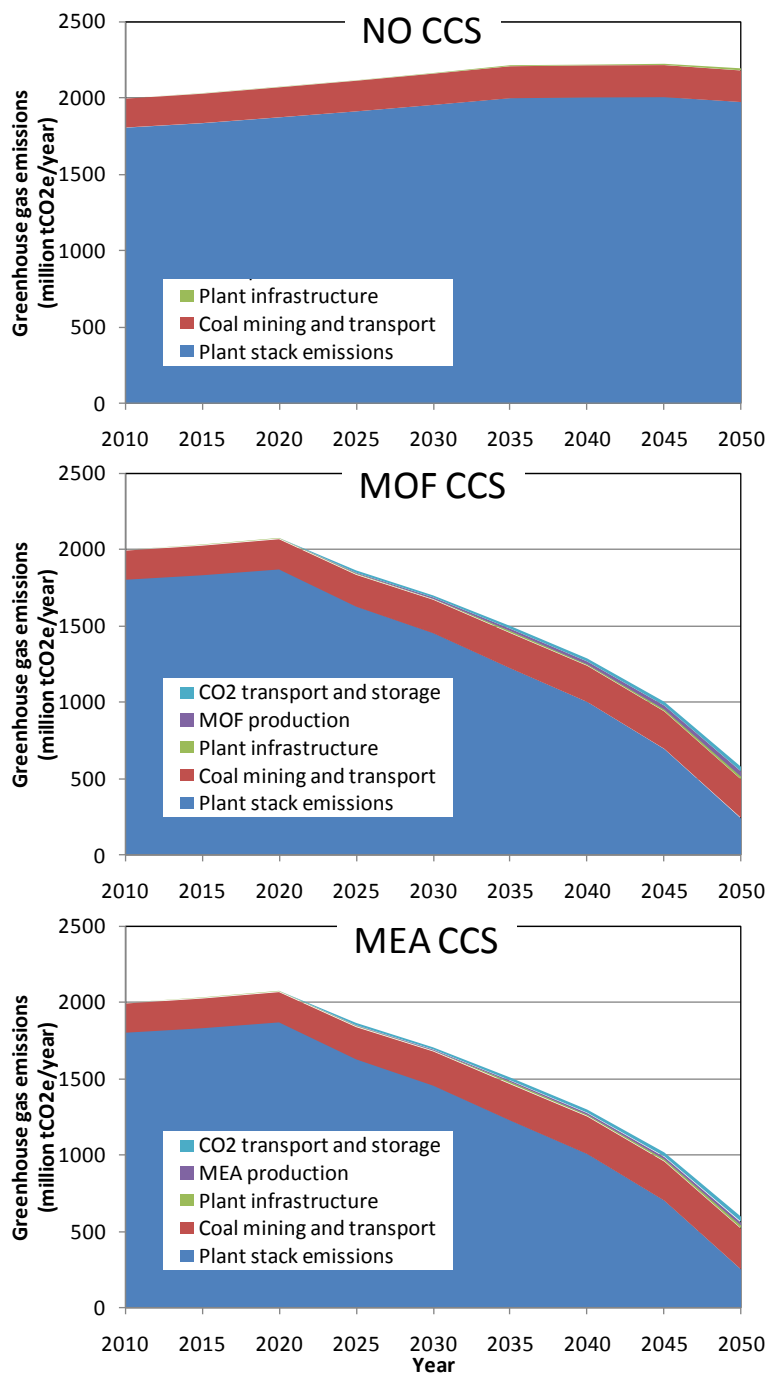


Figure S6. Estimated system-wide GHG emissions (million tCO₂e y⁻¹) from 2010 to 2050 for cases with no CO₂ capture and with MOF- and MEA-based capture systems.

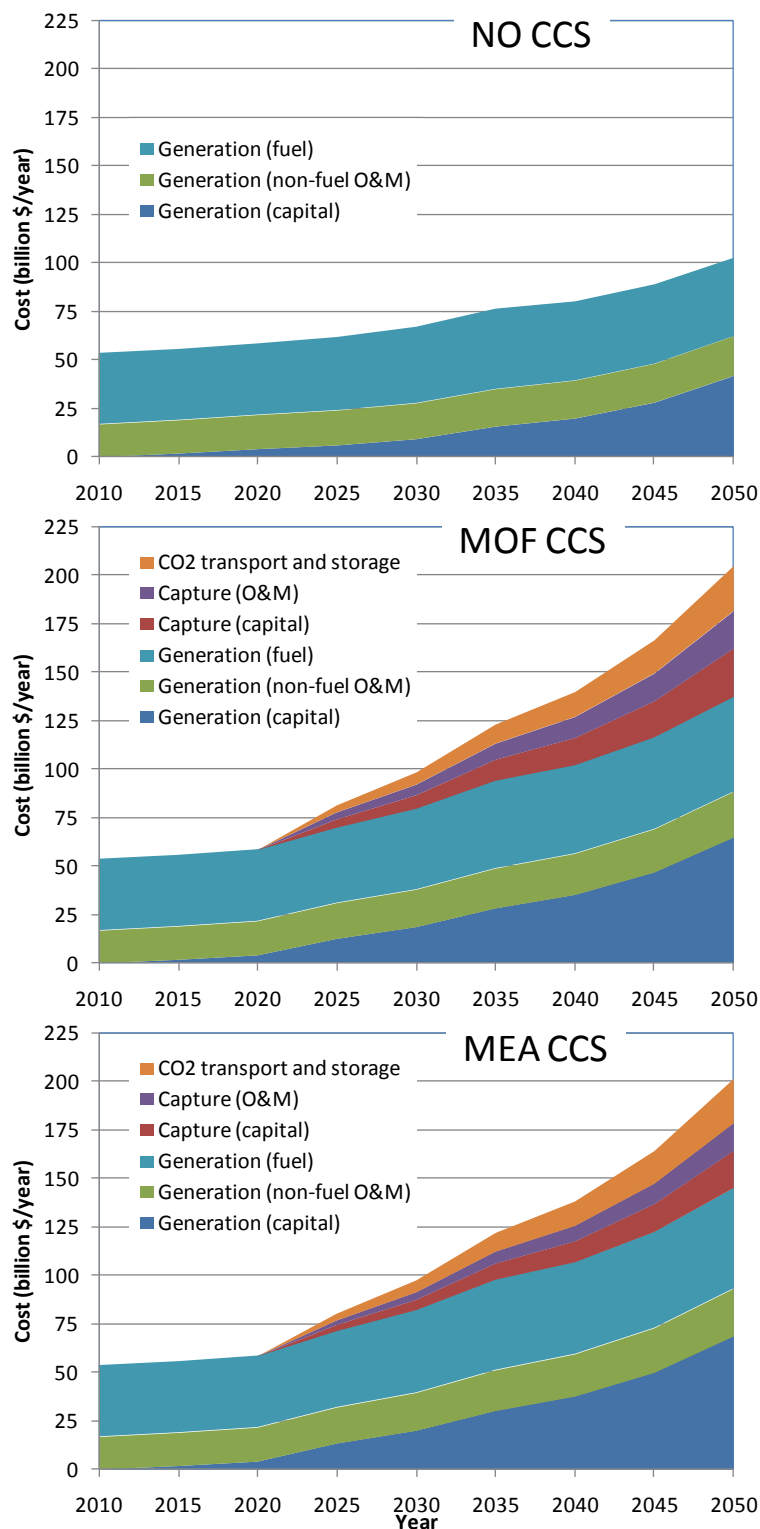


Figure S7. Estimated total system cost ($G\$ y^{-1}$) from 2010 to 2050 for cases with no CO_2 capture and with MOF- and MEA-based capture systems.

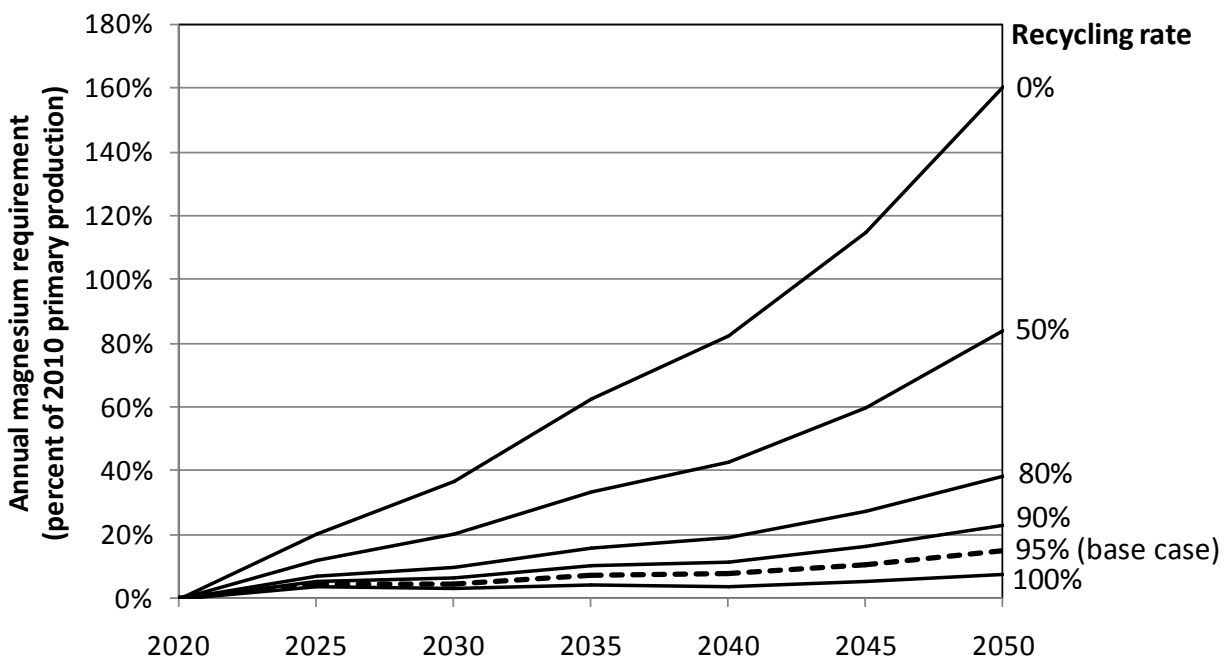


Figure S8. Estimated annual primary metal requirement for MOF production, expressed as a percentage of 2010 primary magnesium production, as a function of recycling rate of metal in post-use MOF material.

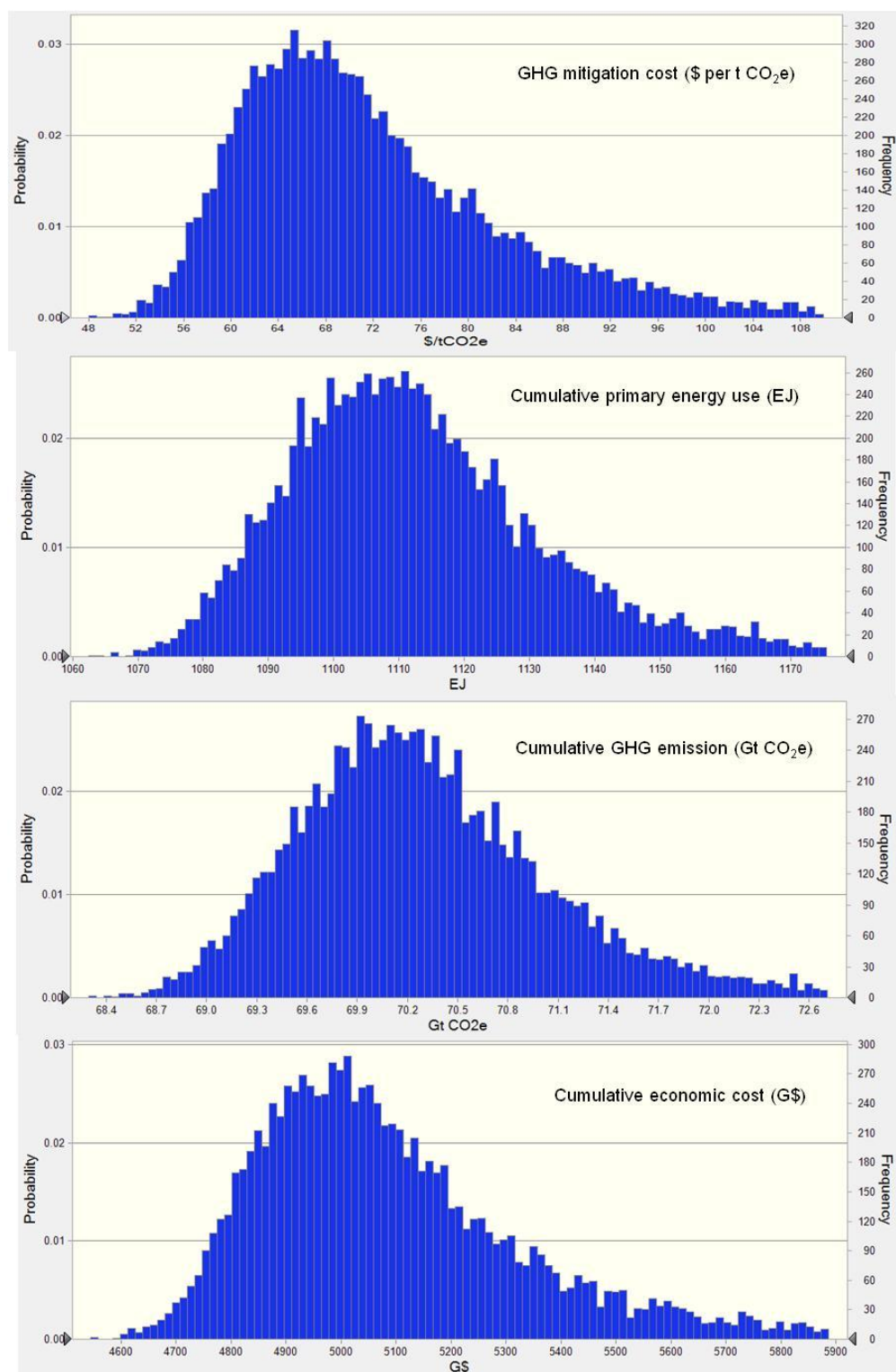


Figure S9. Outcomes of Monte Carlo simulation of full-scale deployment of MOF-based carbon capture and storage in the US coal-fired power fleet through 2050: GHG mitigation cost (\$ per tCO₂e), total cumulative primary energy use (EJ), total cumulative GHG emissions (Gt CO₂e), and total cumulative cost for coal-fired electricity production (G\$).